El Niño/Southern Oscillation (ENSO)

First noticed in time series of pressure, e.g. at Tahiti and Darwin:

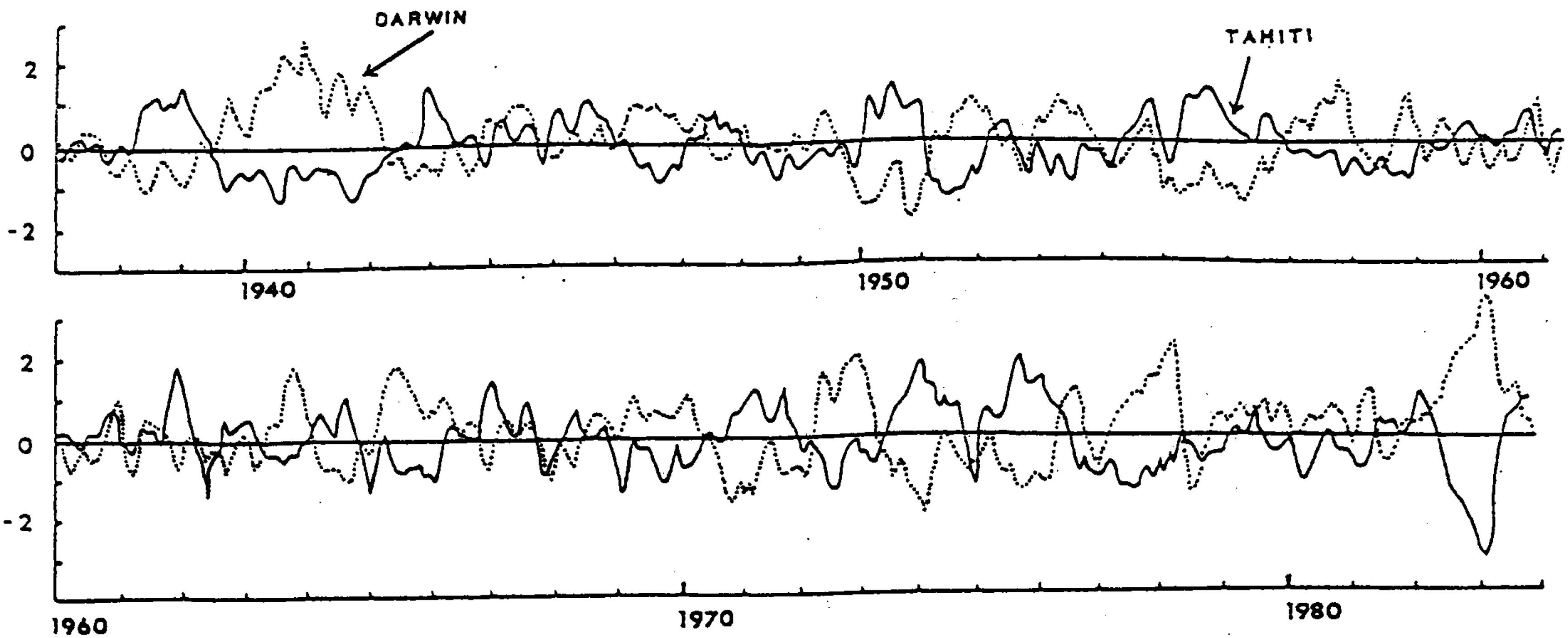

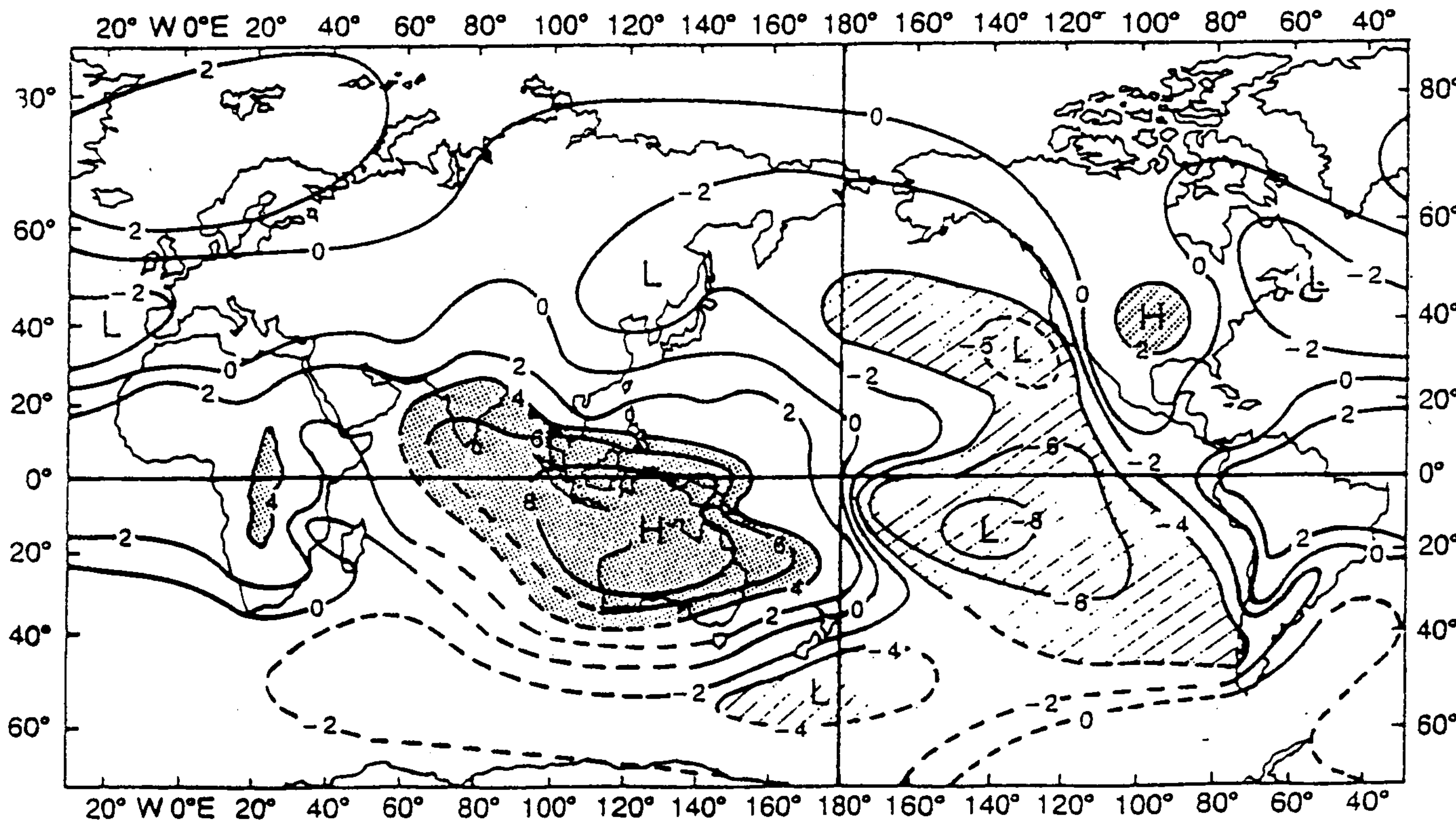

Figure 1.1. Correlations ($\times 10$) of annual mean sea level pressure with the pressure at Darwin. Correlations exceed 0.4 in the shaded regions and are less than -0.4 in the regions th dashed lines. [From Trenberth and Shea (1987).]

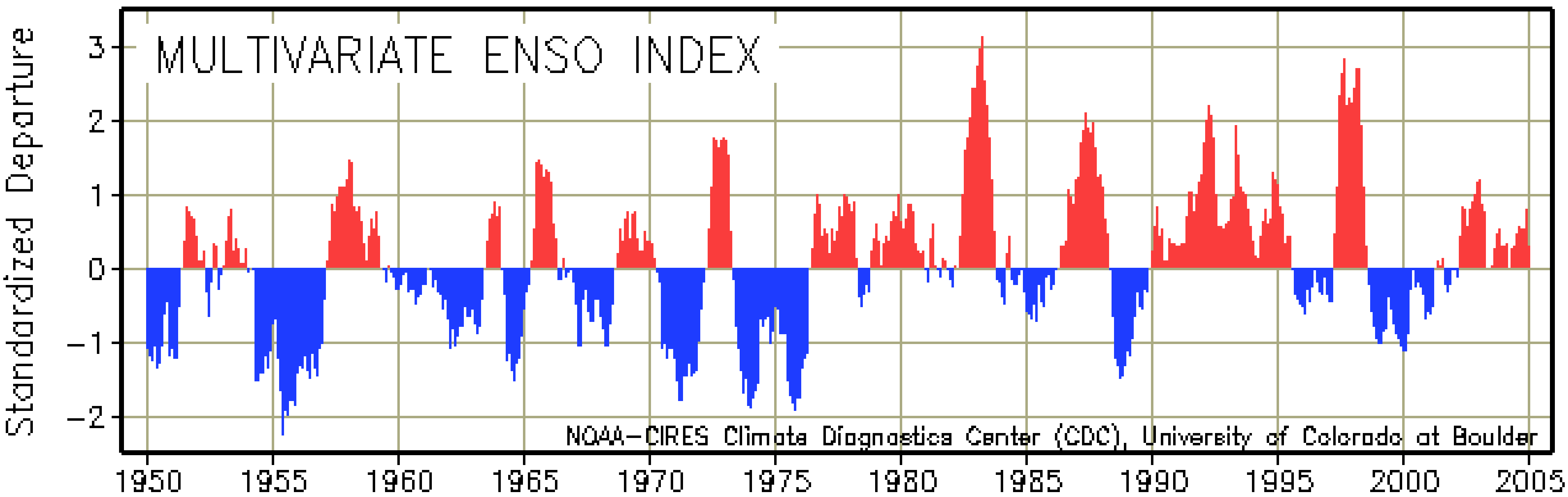
MULTIVARIATE ENSO INDEX
Standardized Departure
3
2
1
0
−1
−2
NOAA-CIRES Climate Diagnostics Center (CDC), University of Colorado at Boulder
1950
1955
1960
1965
1970
1975
1980
1985
1990
1995
2000
2005

Large excursions of SST in central and eastern equatorial Pacific:

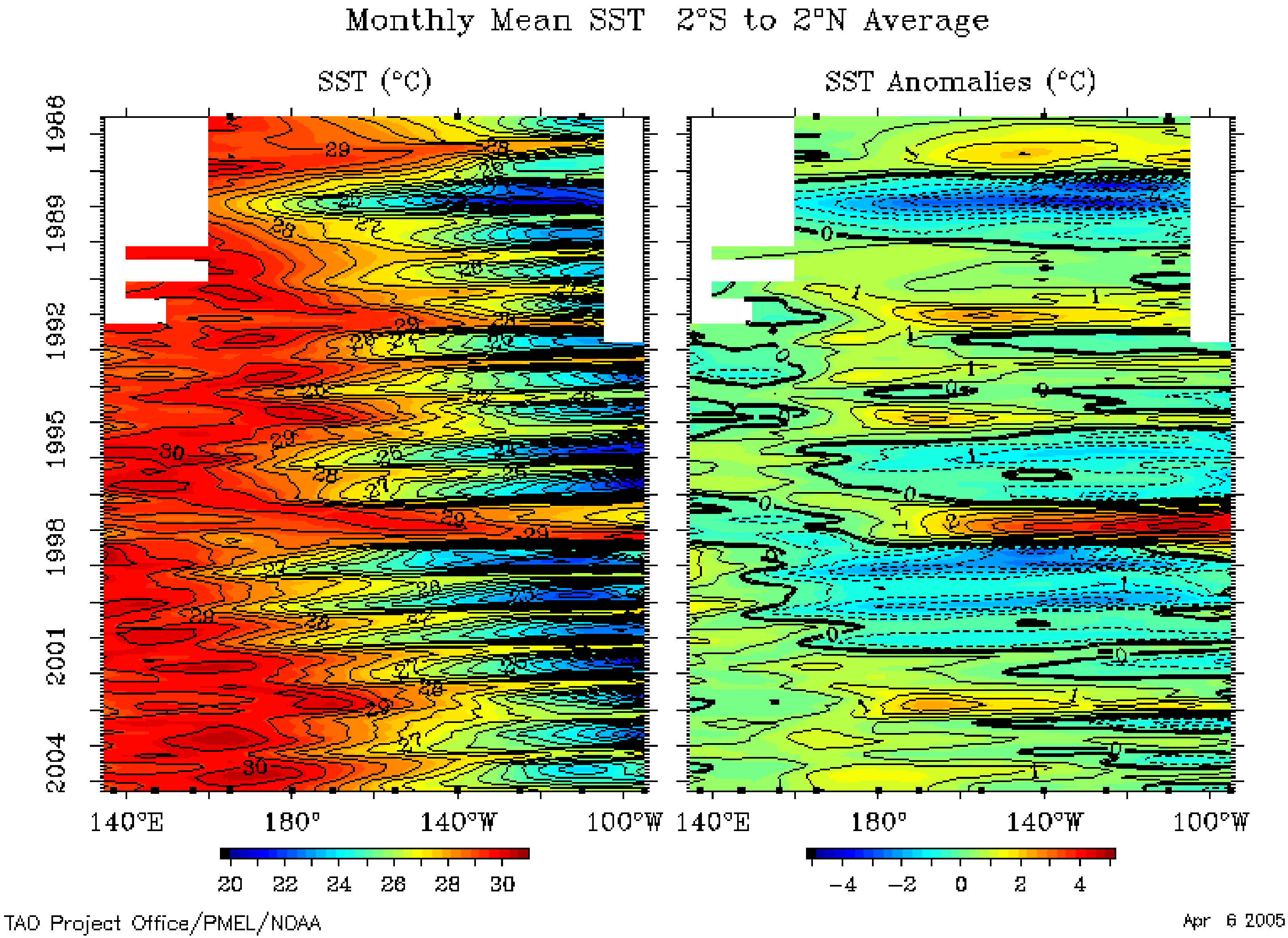

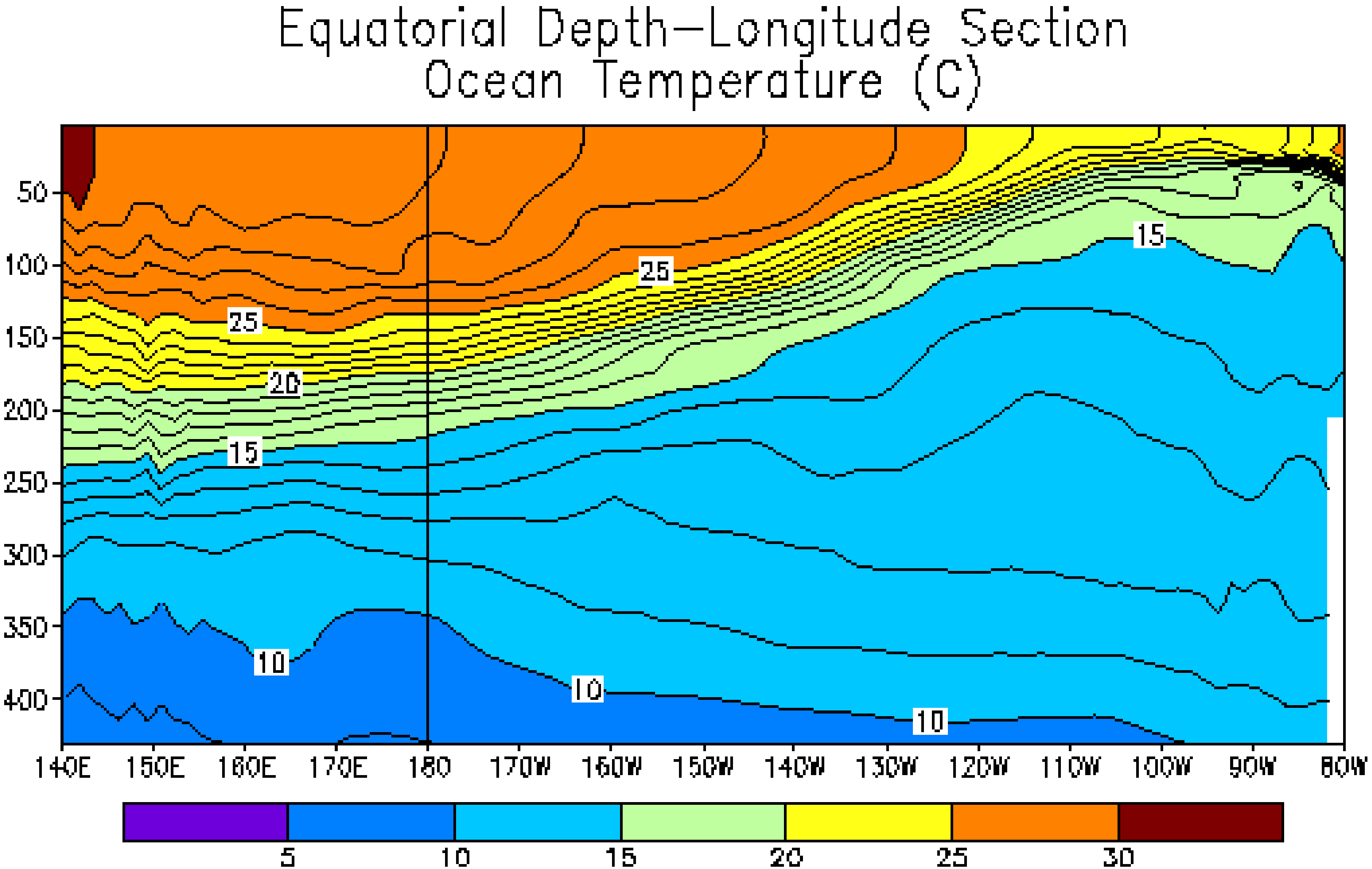
Equatorial Depth-Longitude Section
Ocean Temperature (C)
50
100
150
200
250
300
350
400
140E
150E
160E
170E
180
170W
160W
150W
140W
130W
120W
110W
100W
90W
80W
25
25
20
15
15
10
10
10
5
10
15
20
25
30

Accompanied by large excursions of equatorial thermocline:

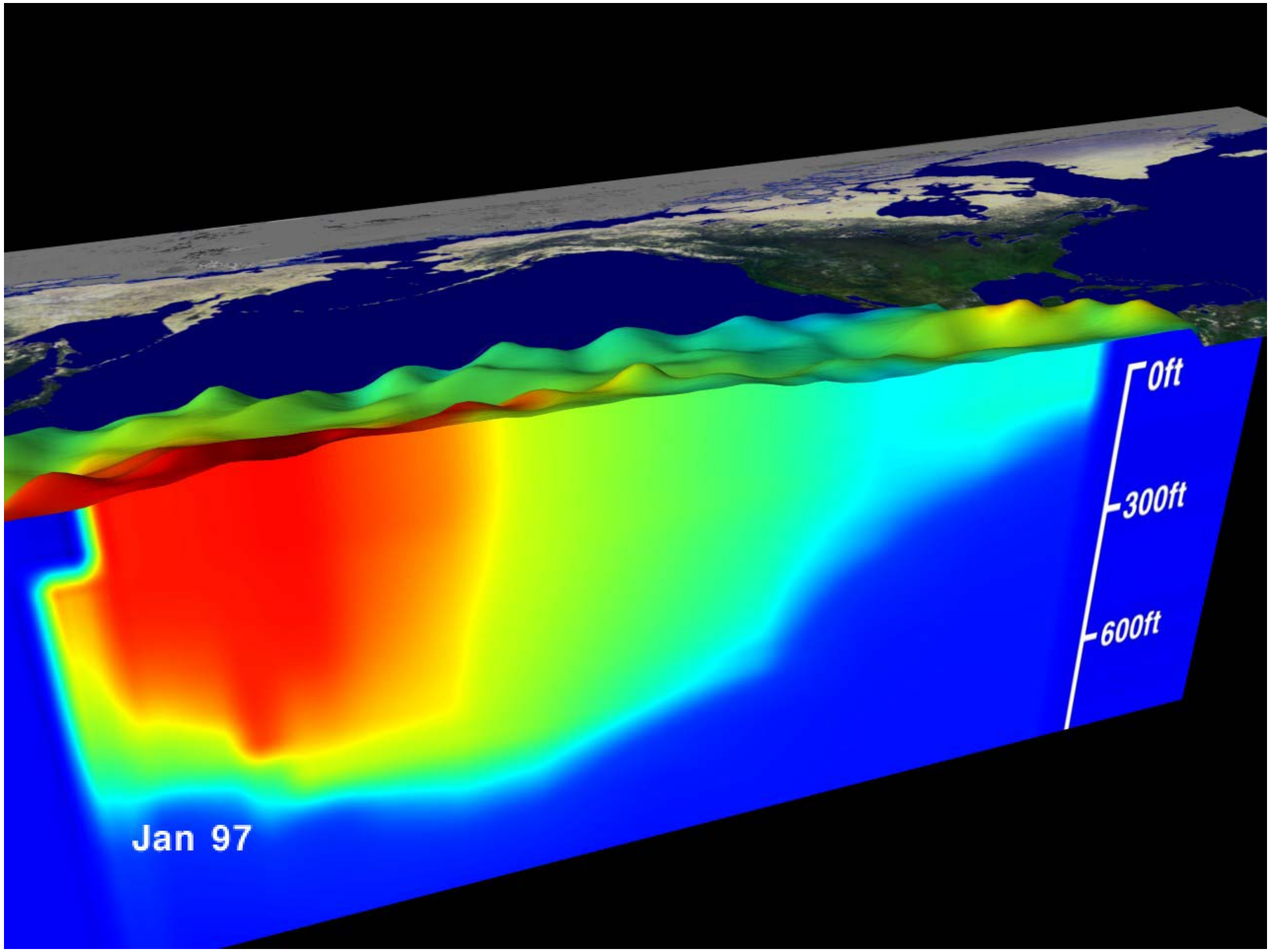

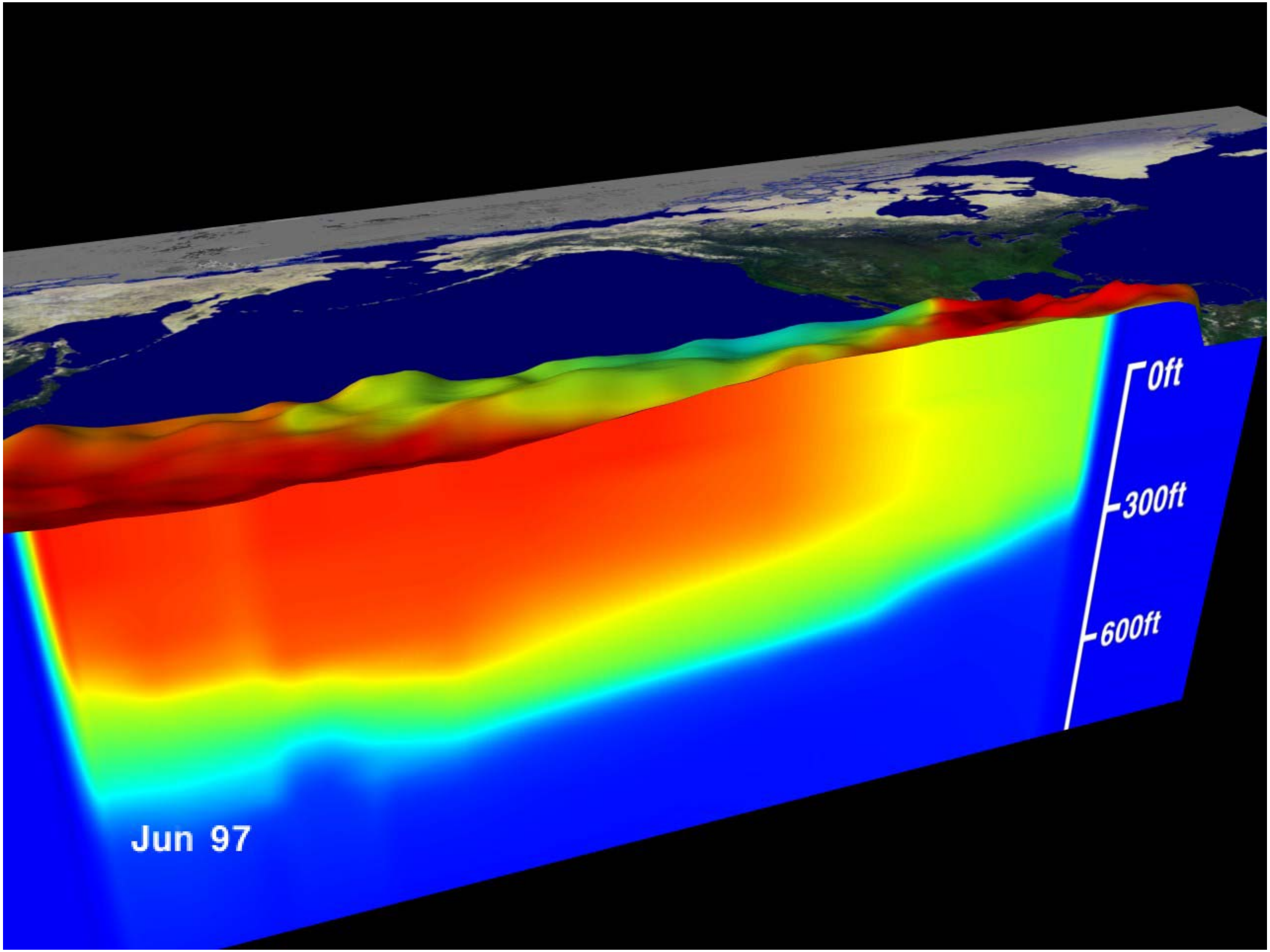
0ft
300ft
600ft
Jun 97

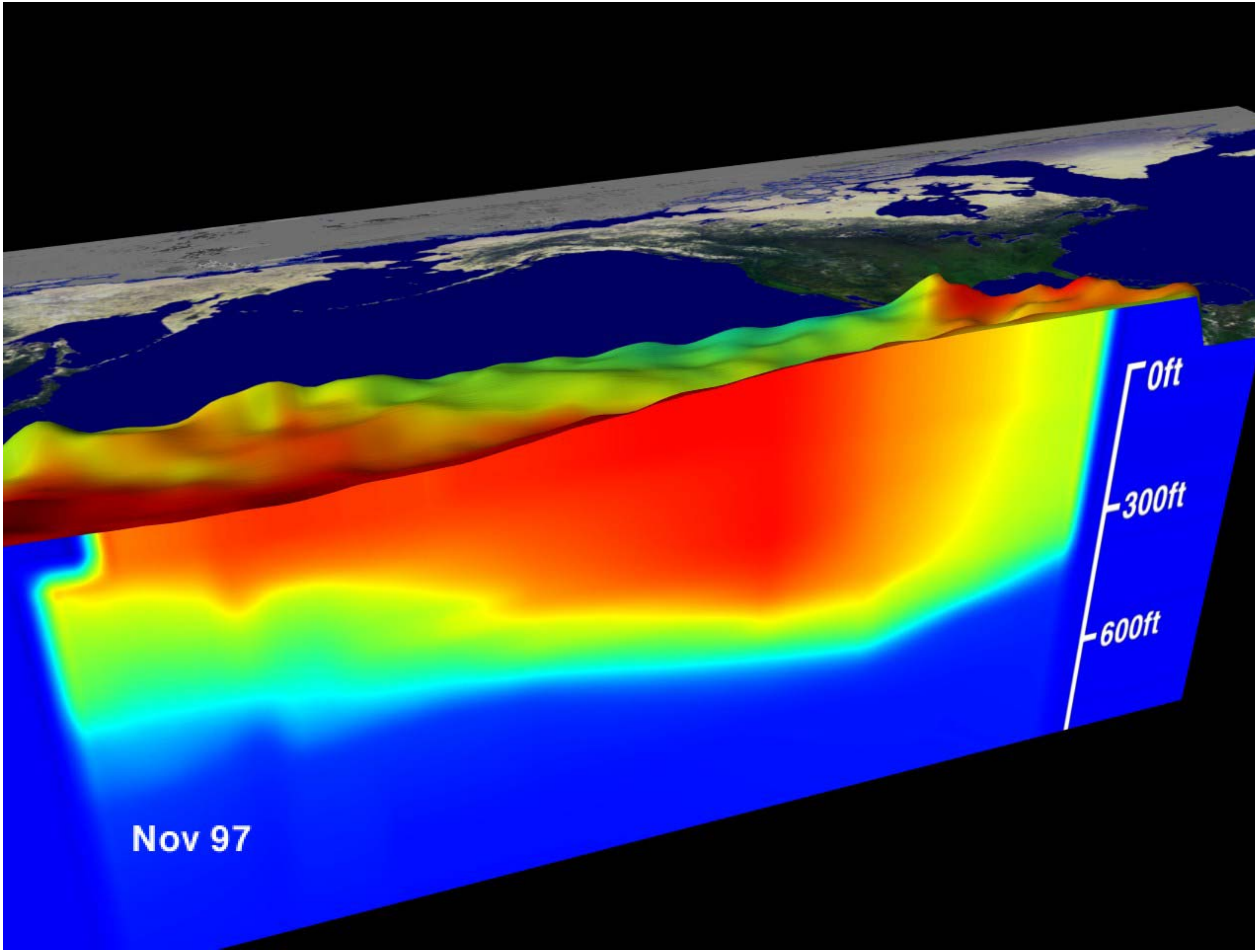
0ft
300ft
600ft
Nov 97

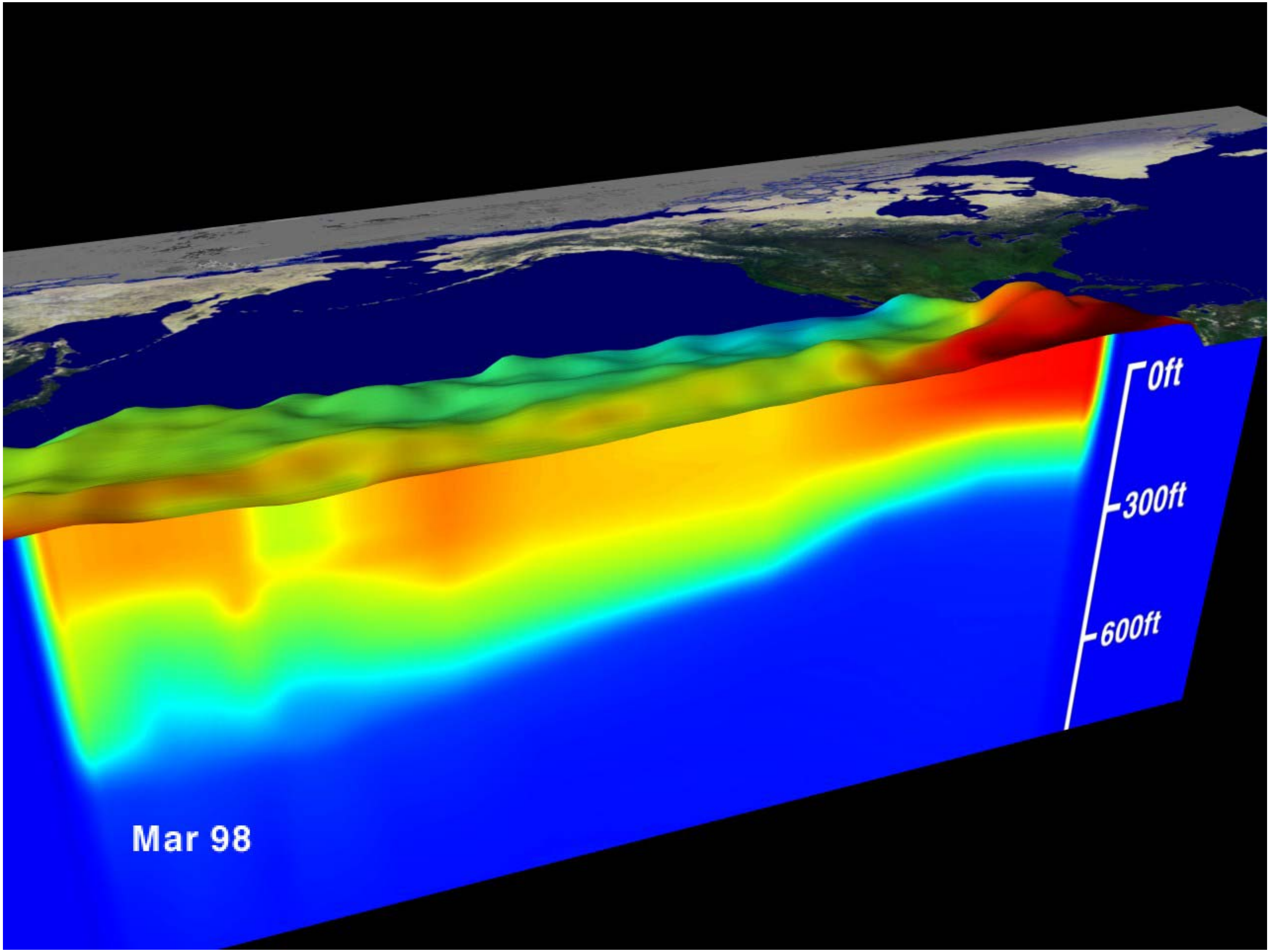
0ft
300ft
600ft
Mar 98

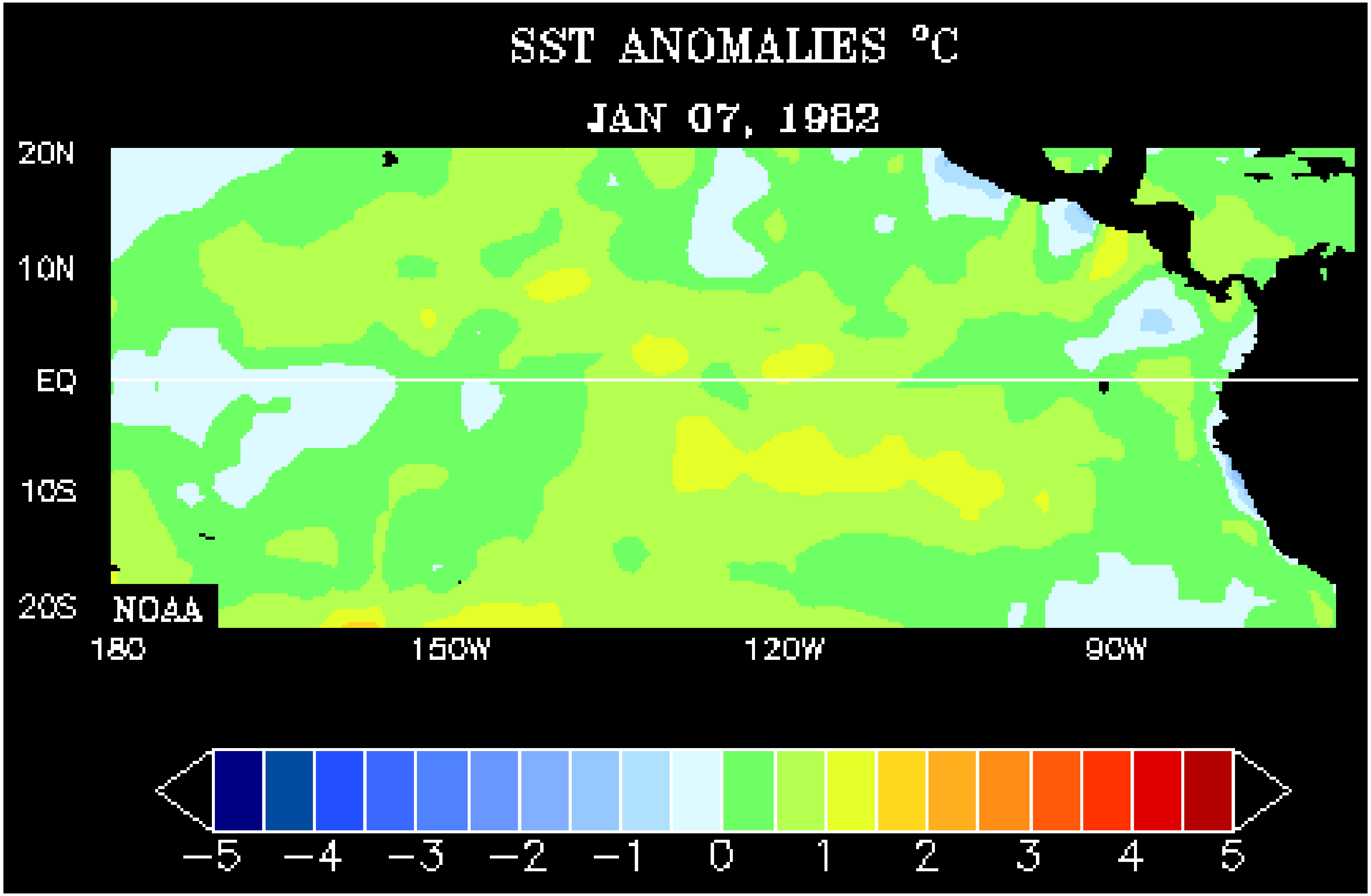
SST ANOMALIES °C
JAN 07, 1982
20N
10N
EQ
10S
20S
NOAA
180
150W
120W
90W
−5 −4 −3 −2 −1 0 1 2 3 4 5

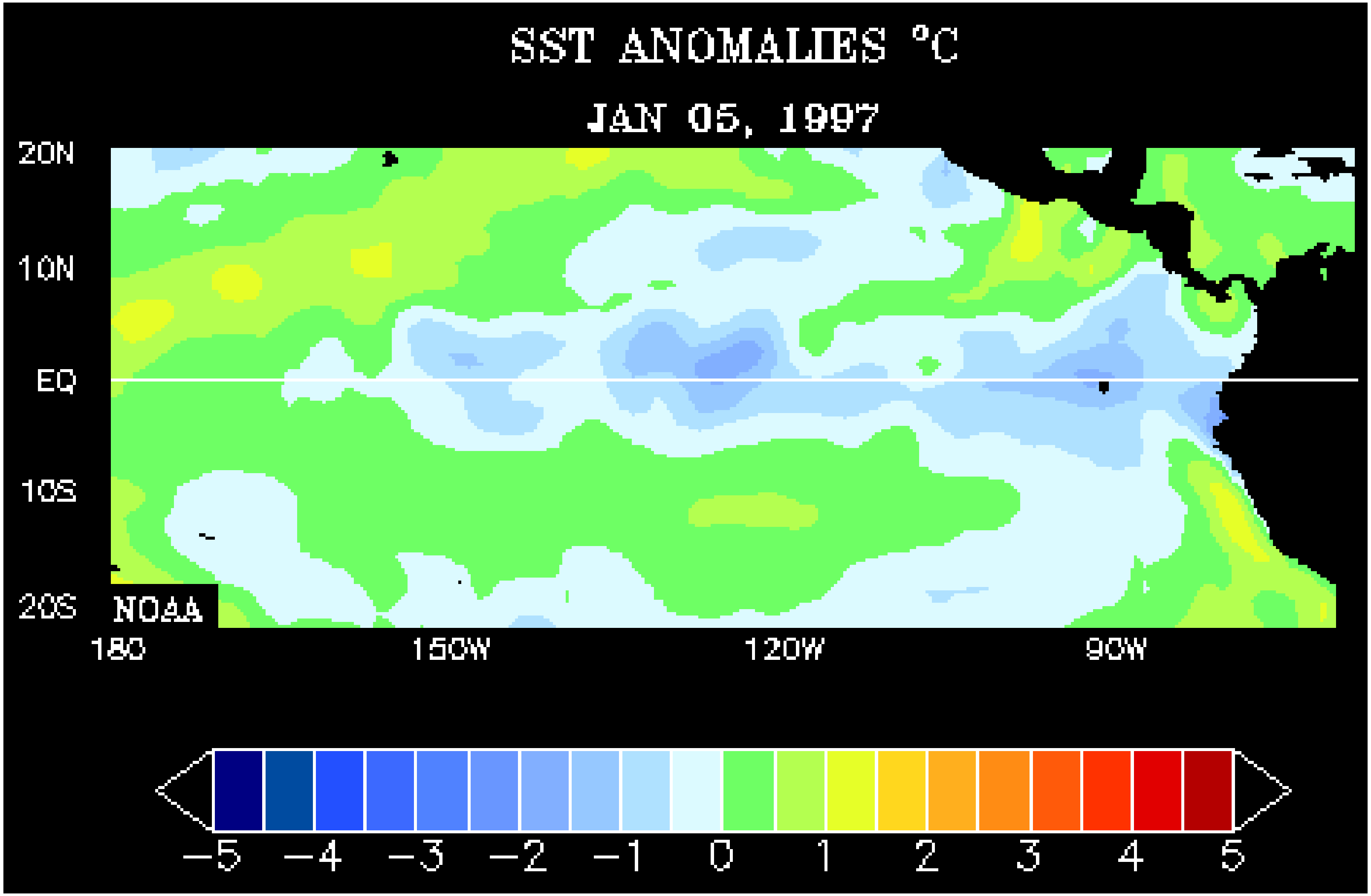

SST ANOMALIES °C
JAN 05, 1997
20N
10N
EQ
10S
20S
NOAA
180
150W
120W
90W
−5
−4
−3
−2
−1
0
1
2
3
4
5

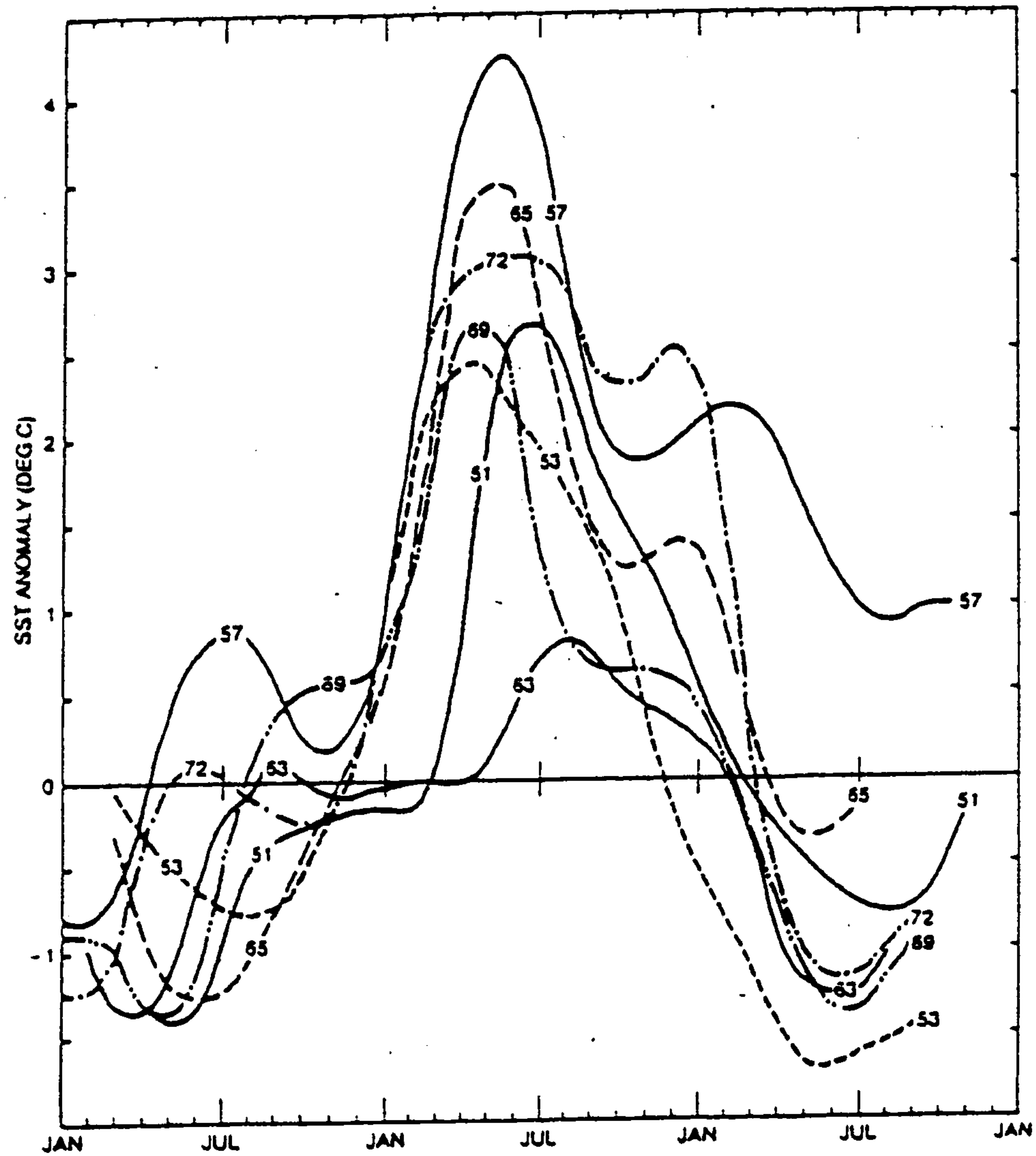

FIG. 10. SST(1) anomaly time series for the seven most significant warm episodes between 1950 and 73.

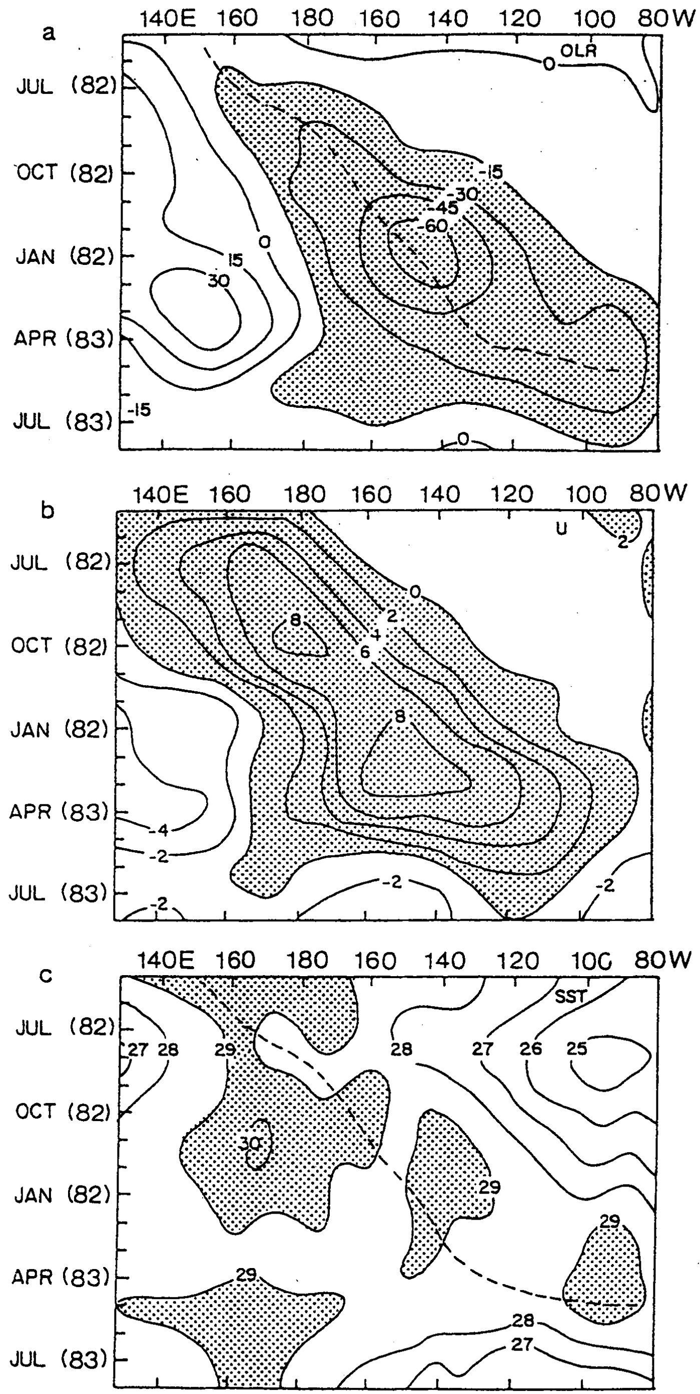

OLR

Westerly wind

SST

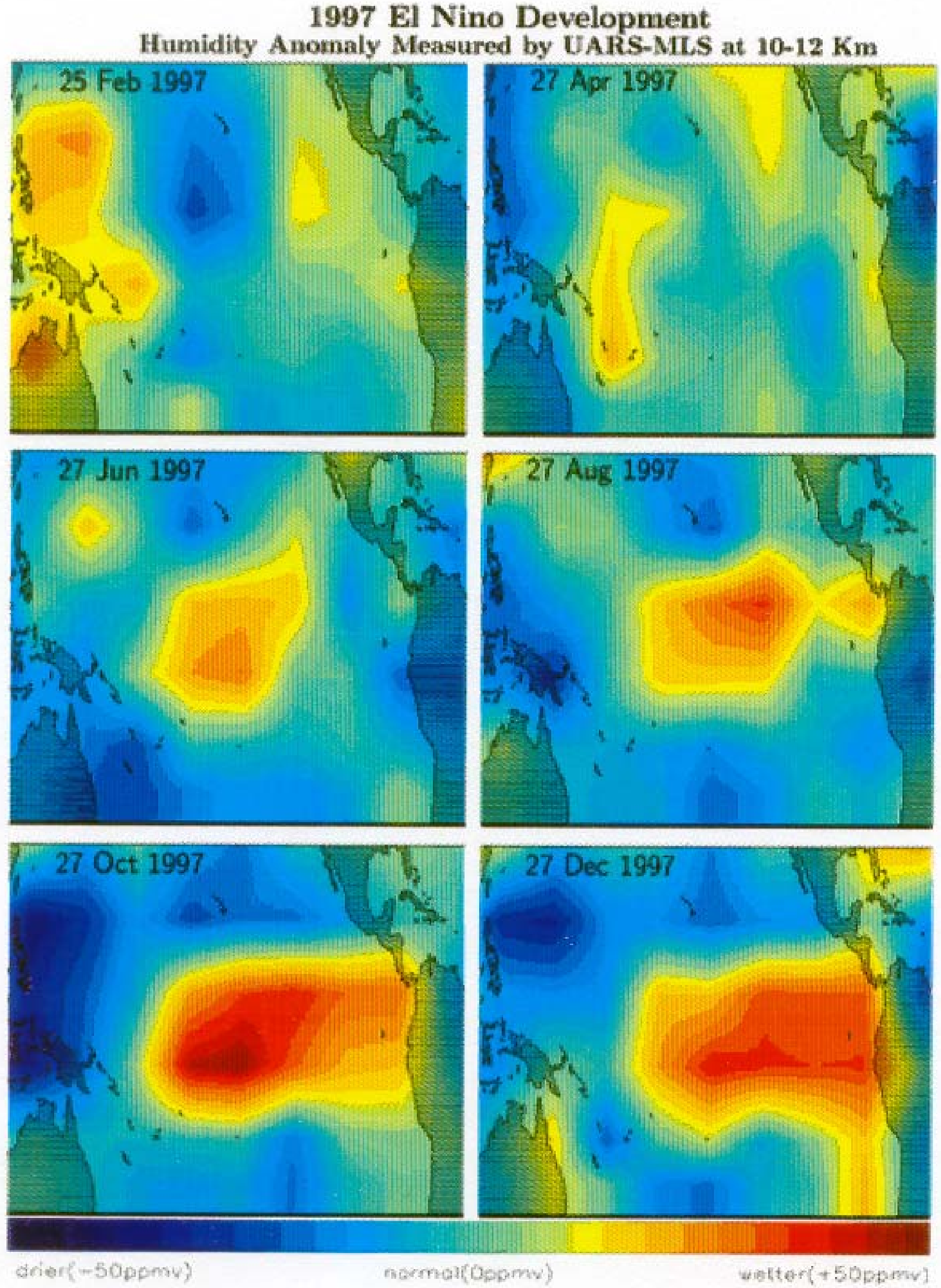

UARS humidity anomaly

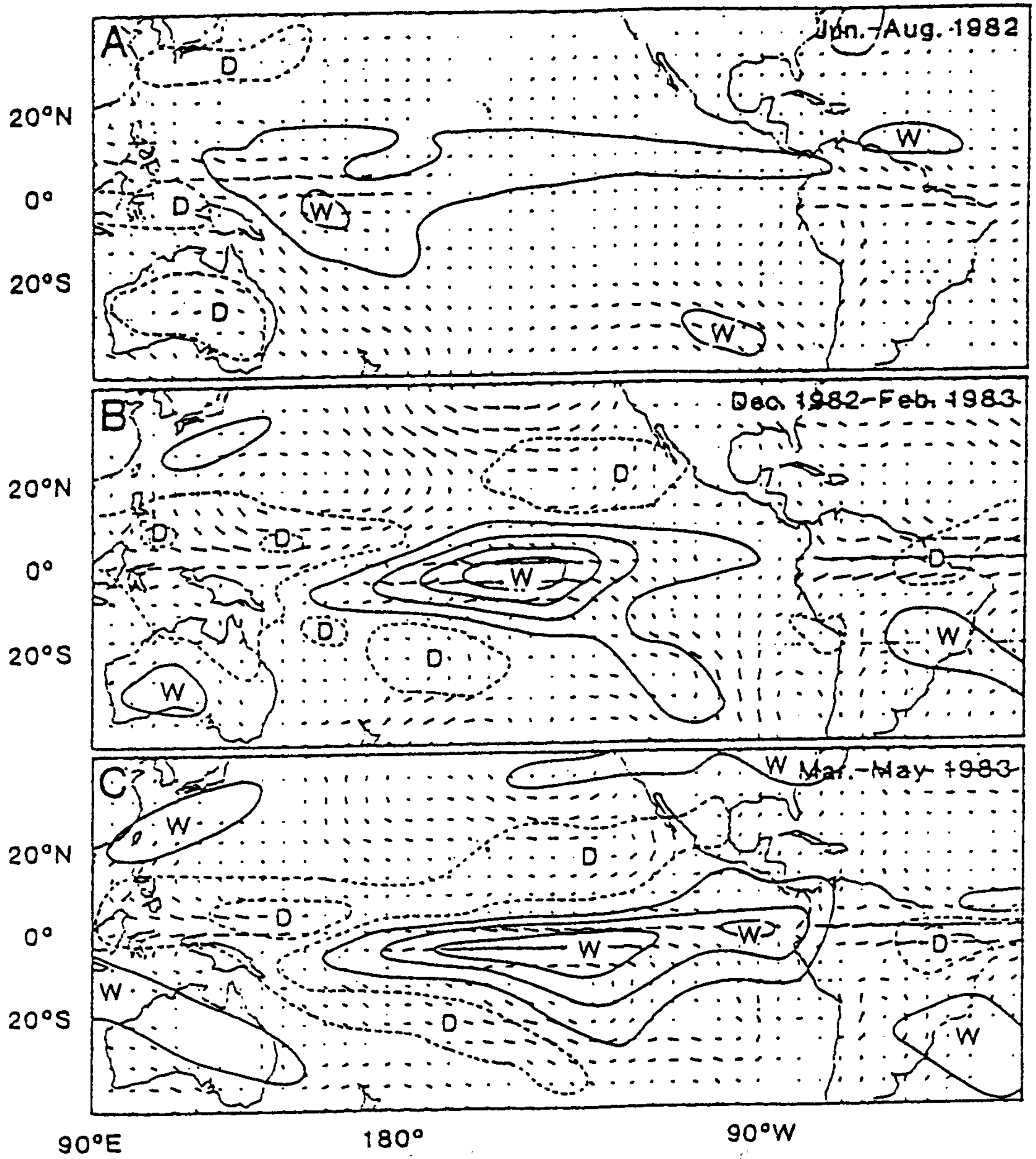

OLR and
850 hPa
wind

Evolution of SST and surface winds

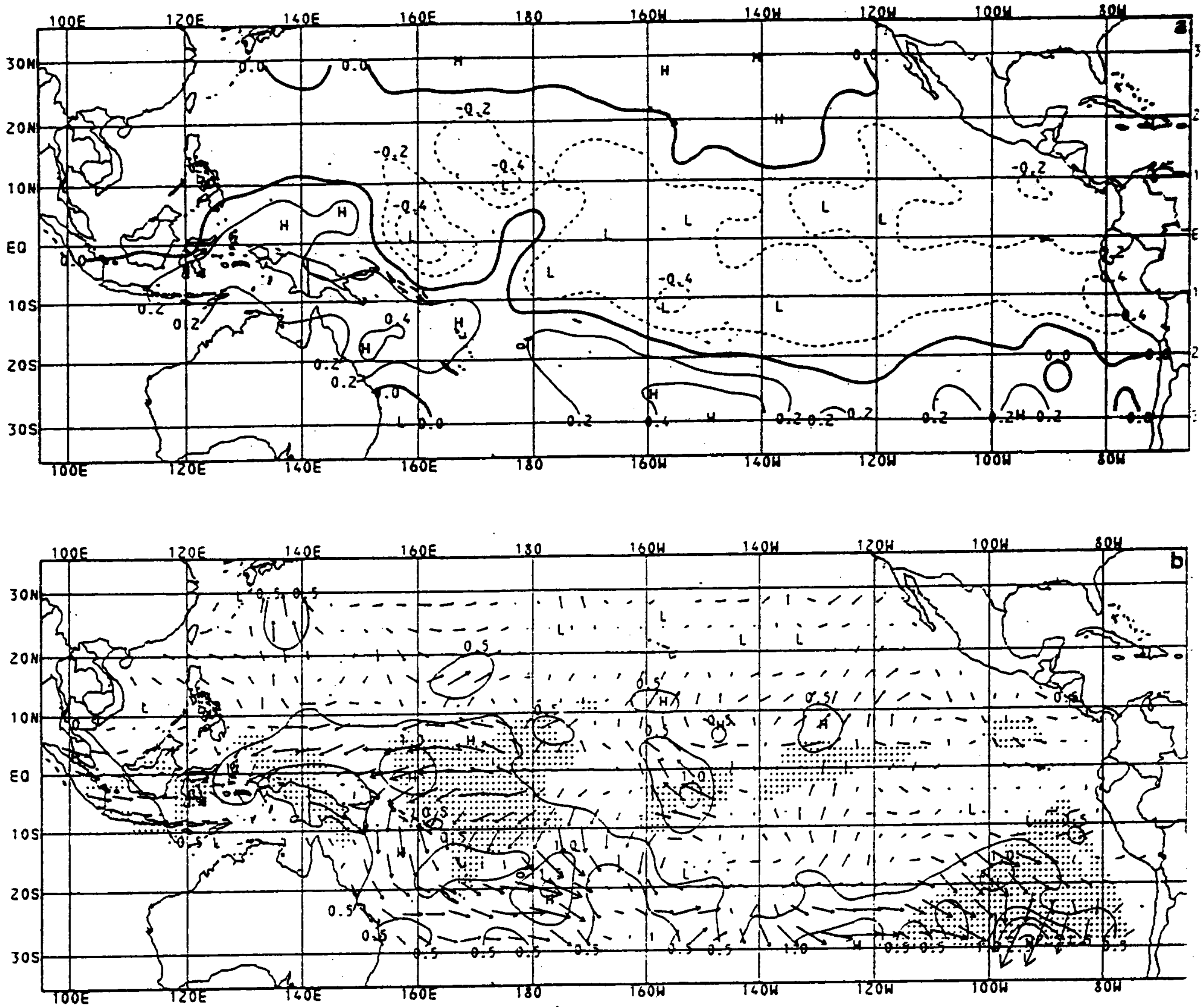

Preceding August-October

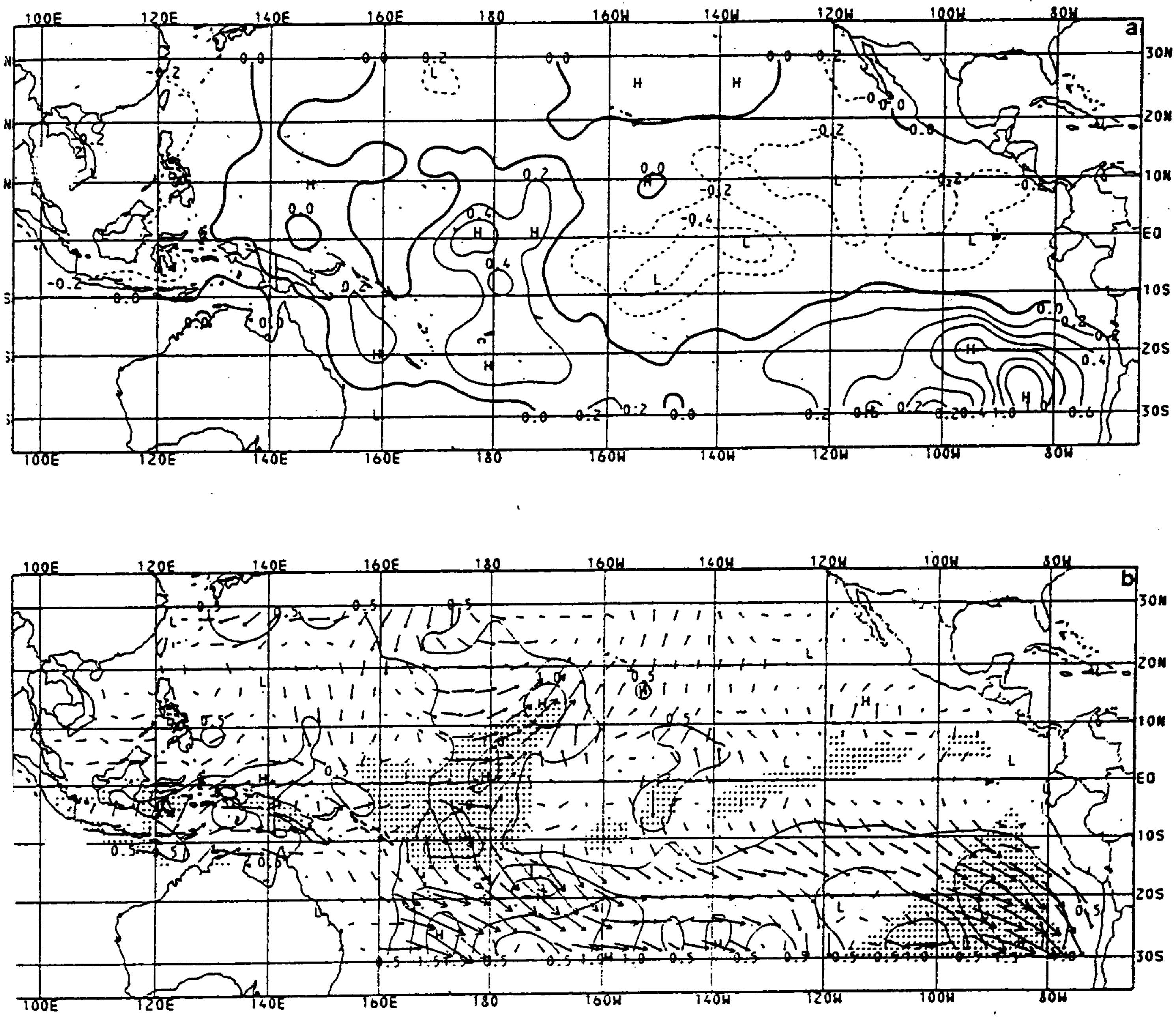

Preceding November -January

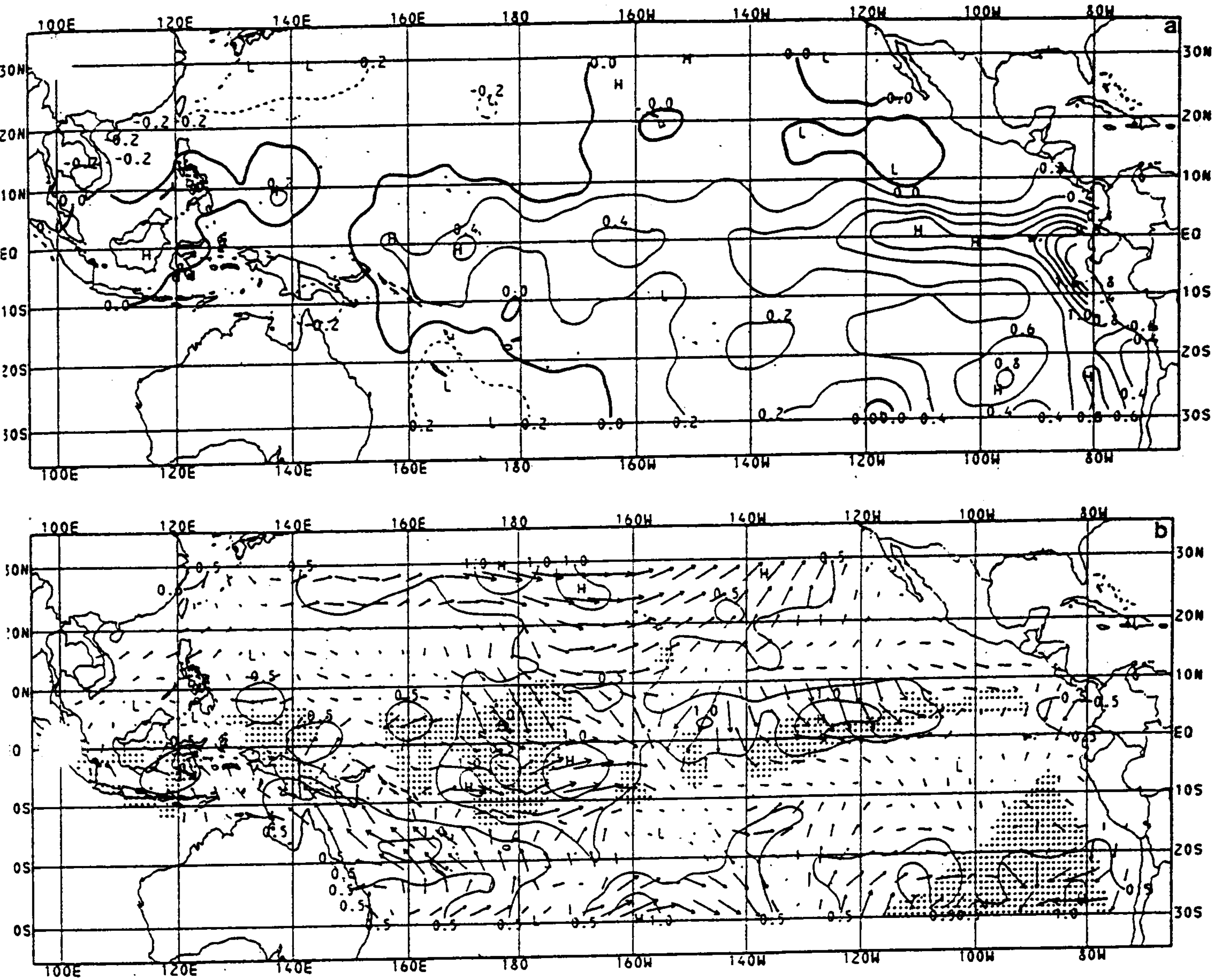
a
b
100E
120E
140E
160E
180
160W
140W
120W
100W
80W
30N
20N
10N
EQ
10S
20S
30S

March-
May

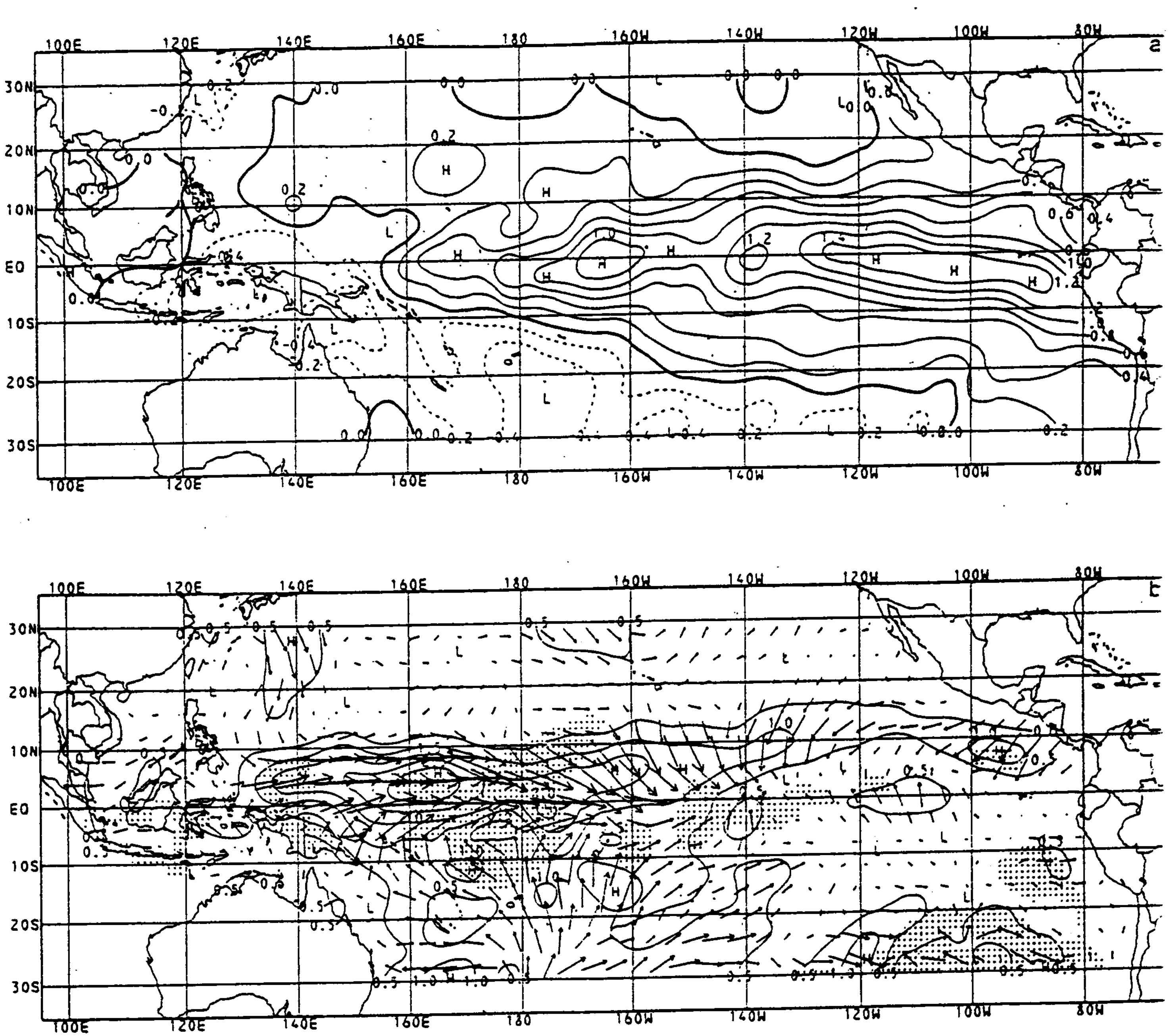

August-October

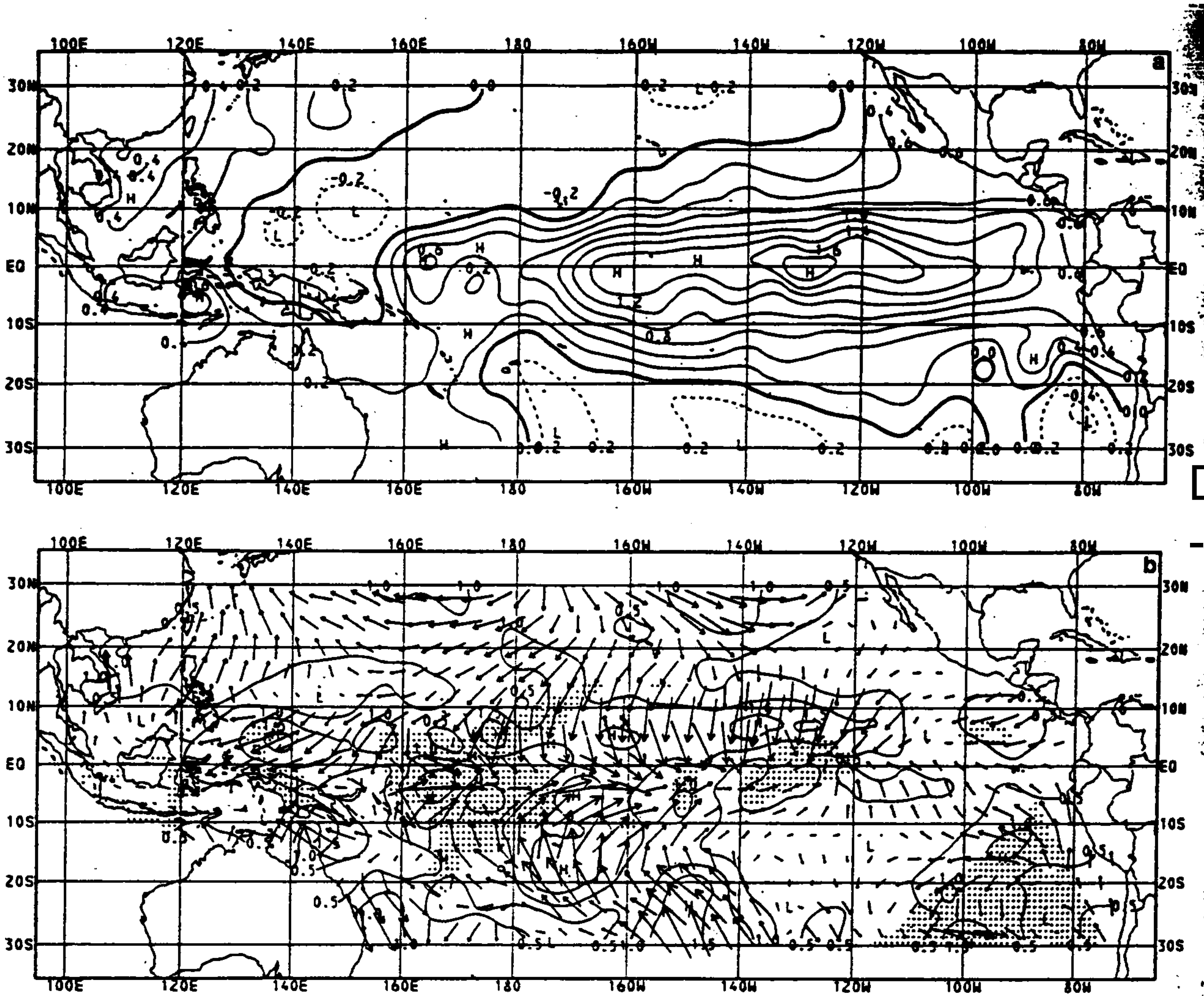

December
-February

La Niña Conditions

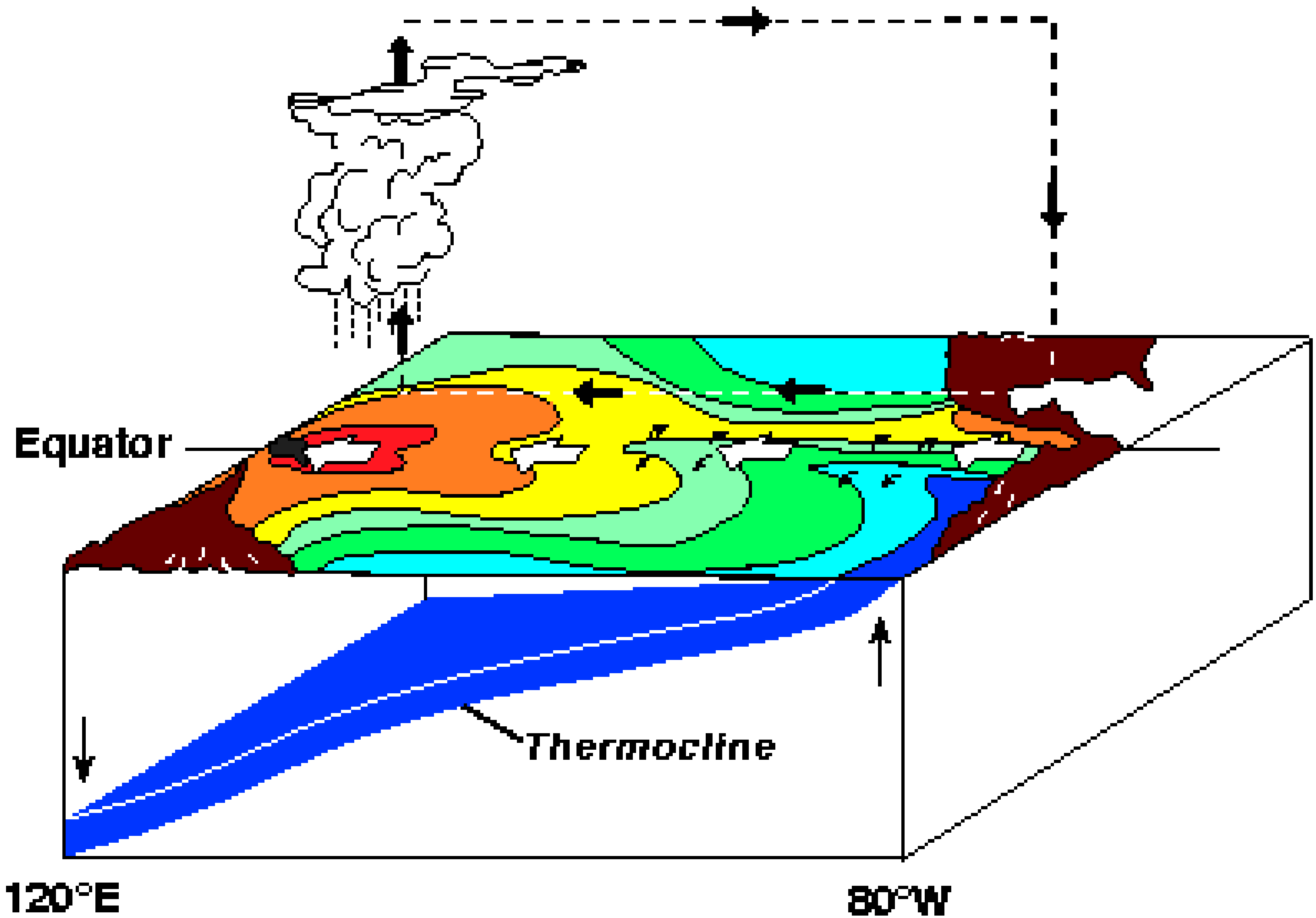

Normal Conditions

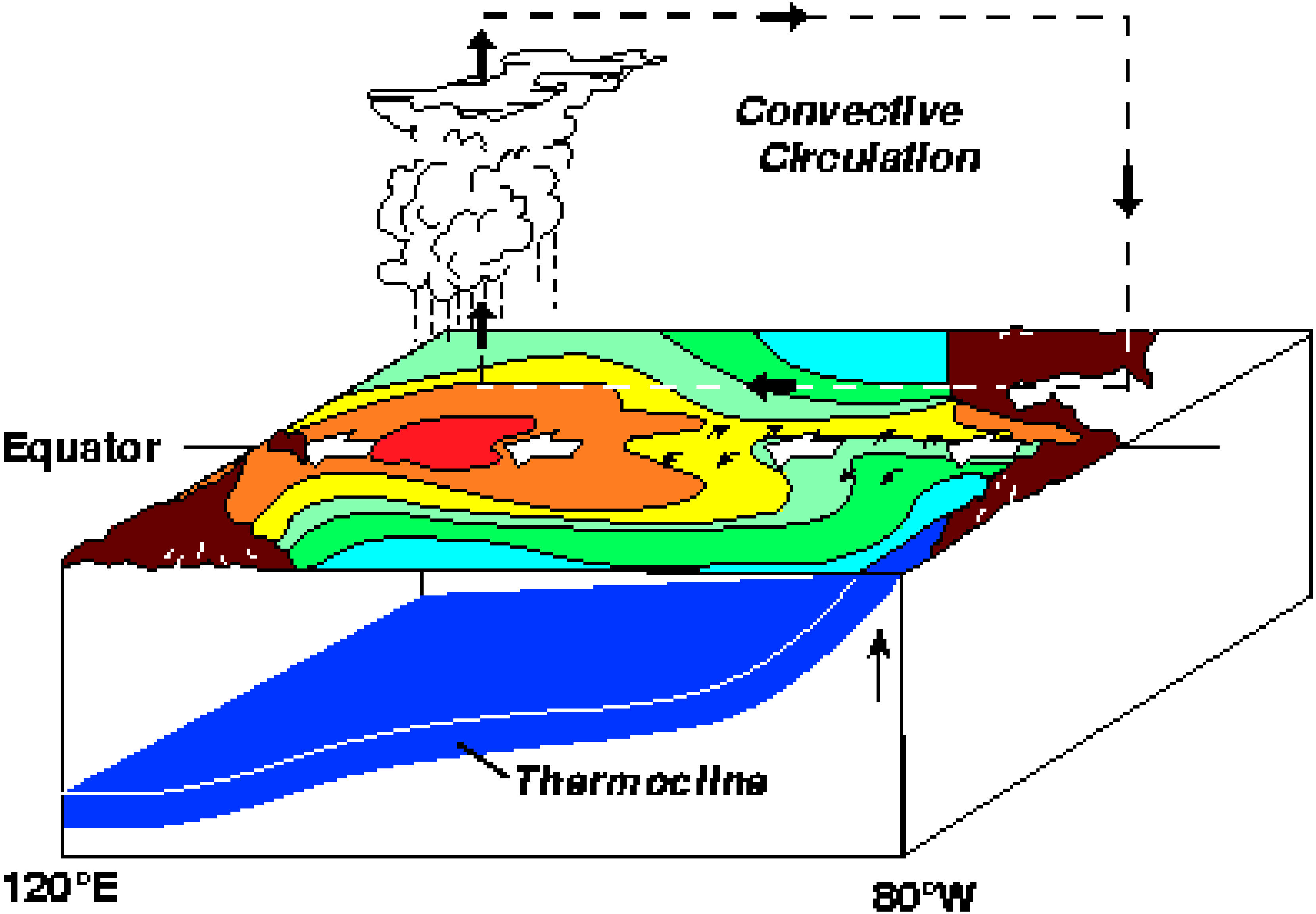

El Niño Conditions

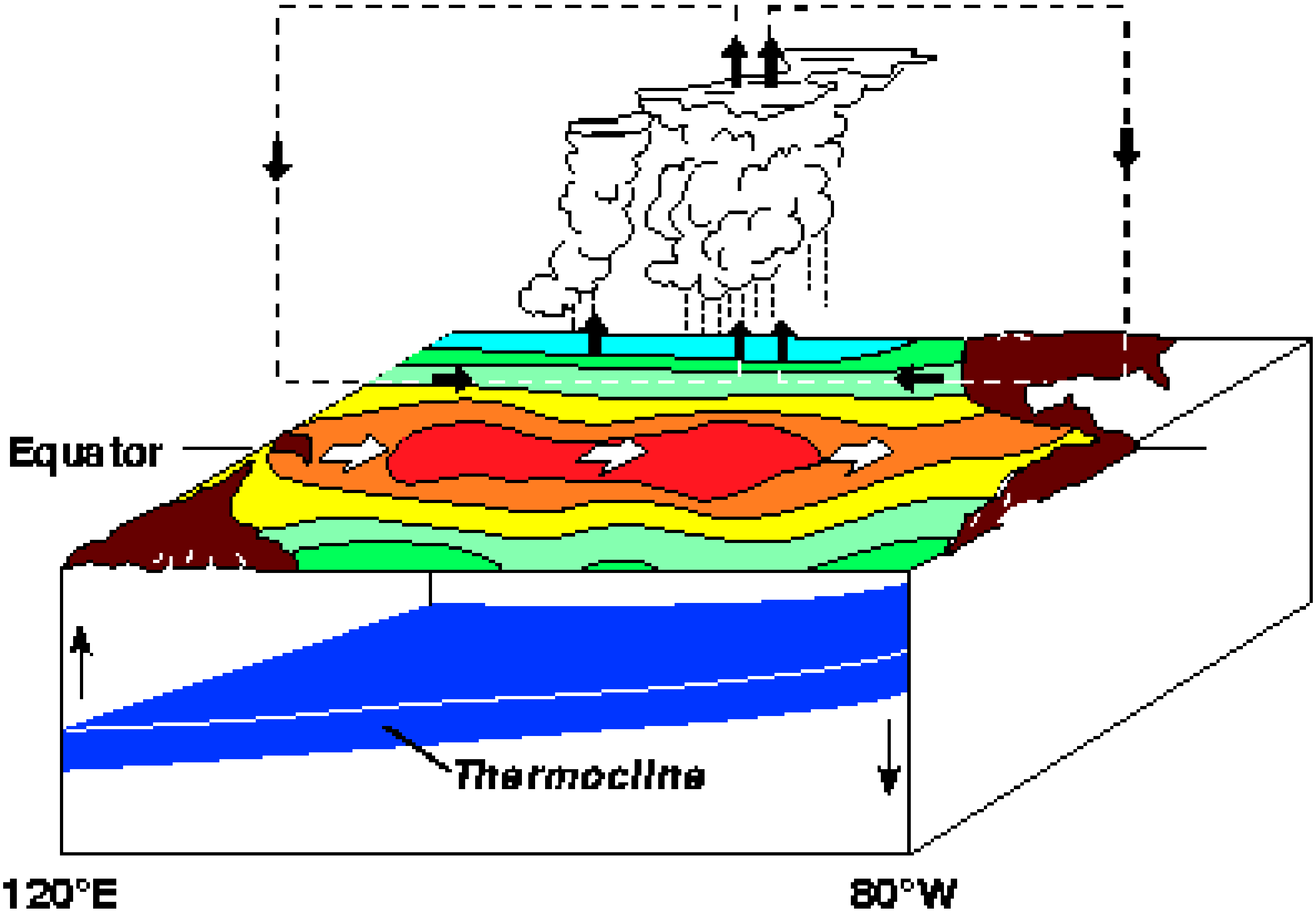

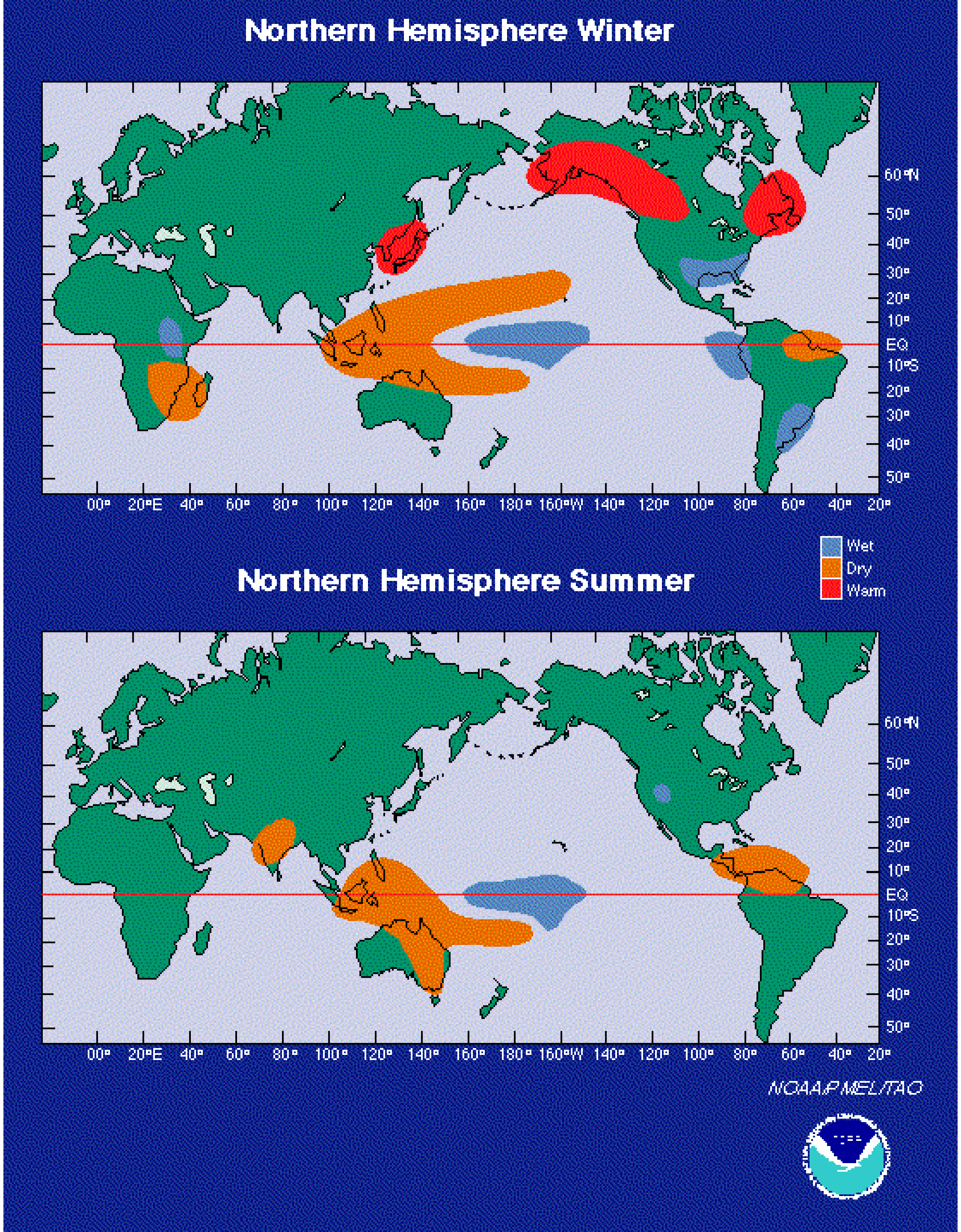

Northern Hemisphere Winter
60°N
50°
40°
30°
20°
10°
EQ
10°S
20°
30°
40°
50°
00° 20°E 40° 60° 80° 100° 120° 140° 160° 180° 160°W 140° 120° 100° 80° 60° 40° 20°
Wet
Dry
Warm
Northern Hemisphere Summer
60°N
50°
40°
30°
20°
10°
EQ
10°S
20°
30°
40°
50°
00° 20°E 40° 60° 80° 100° 120° 140° 160° 180° 160°W 140° 120° 100° 80° 60° 40° 20°
NOAA/PMEL/TAO

Main Issues (contributed by E. Tziperman):

- What is the mechanism of the El Nino cycle?
- Why is the mean period quite robustly 4 years?
- Is ENSO self-sustained or is it damped and requires external forcing by weather noise for example in order to be excited?
- Why are ENSO events irregular: is it due to chaos? noise?
- Why do ENSO events tend to peak toward the end of the calendar year (phase locking to the seasonal cycle)?

ENSO Theory

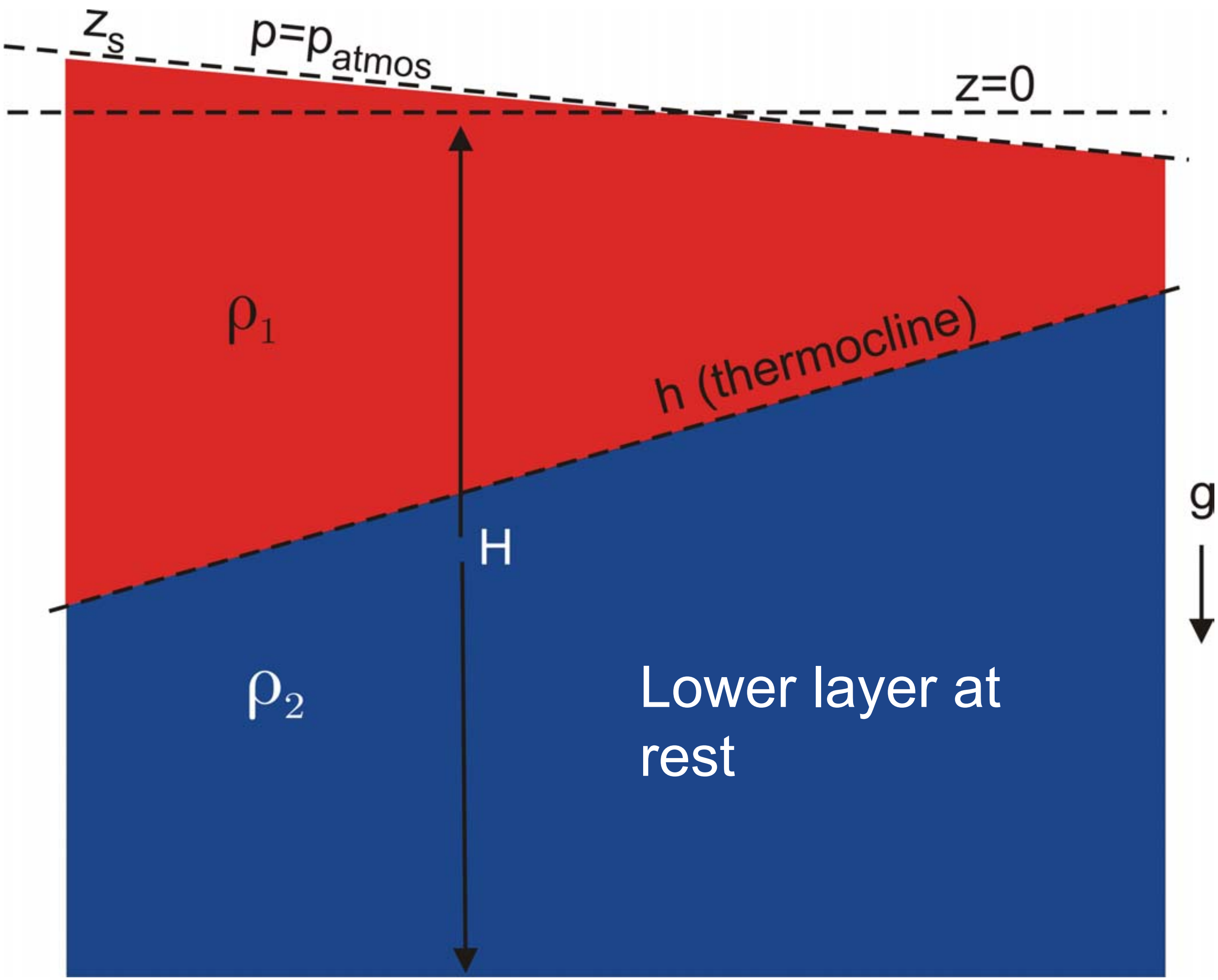

$$p_H = constant = p_{atmos} + \rho_1 g\left(h + z_s\right) + \rho_2 g\left(H - h\right)$$
$$\rightarrow h\left(\rho_1 - \rho_2\right) + z_s \rho_1 = constant$$

Hydrostatic: At fixed depth within layer 1:

$$p = p_{atmos} + \rho_1 g\left(z + z_s\right)$$
$$\rightarrow \frac{1}{\rho_1}\nabla p = g\nabla z_s = g\frac{\rho_2 - \rho_1}{\rho_1}\nabla h \equiv g^*\nabla h$$

$$\frac{d\mathbf{V}}{dt} + \beta y\hat{k}\times\mathbf{V} + g^*\nabla h = \frac{\boldsymbol{\tau}_s}{\rho_1 h} - \varepsilon_m\mathbf{V}$$

Mass continuity:

$$\int_{-h}^{z_s}\left(\nabla \bullet \mathbf{V} + \frac{\partial w}{\partial z}\right)dz = 0$$

$$\rightarrow \frac{dh}{dt} + h\nabla \bullet \mathbf{V} \cong 0$$

Linear shallow water system:

$$\frac{\partial u}{\partial t} - \beta y v + g^* \frac{\partial h}{\partial x} = \frac{\tau_x}{\rho H} - \varepsilon_m u,$$

$$\frac{\partial v}{\partial t} + \beta y u + g^* \frac{\partial h}{\partial y} = \frac{\tau_y}{\rho H} - \varepsilon_m v,$$

$$\frac{\partial h}{\partial t} + H\left(\frac{\partial u}{\partial x} + \frac{\partial v}{\partial y}\right) = -\varepsilon_h h$$

“relaxation term”

Steady, undamped flow at equator:

$$g^* \frac{\partial h}{\partial x} = \frac{\tau_x}{\rho H}$$

Easterly wind gives decreasing thermocline depth toward east. Shallower thermocline is generally associated with colder surface temperatures

For simplicity, take $\varepsilon_m = \varepsilon_h \equiv \varepsilon$

Curl of momentum equations:

$$\left(\frac{\partial}{\partial t} + \varepsilon\right)\left(\frac{\partial v}{\partial x} - \frac{\partial u}{\partial y} - \frac{\beta y h}{H}\right) + \beta v = \hat{k} \bullet \nabla \times \frac{\boldsymbol{\tau}_s}{\rho H}$$

Small variability and damping:

$$\beta v \simeq \hat{k} \bullet \nabla \times \frac{\boldsymbol{\tau}_s}{\rho H}$$ Sverdrup balance

$$\frac{\partial u}{\partial x} \simeq -\frac{\partial v}{\partial y}$$

Steady, undamped flow:

$$g^*\frac{\partial h}{\partial x}=\frac{\tau_x}{\rho H}+\beta yv$$

$$=\frac{\tau_x}{\rho H}-y\frac{1}{\rho H}\frac{\partial \tau_x}{\partial y}$$

Suppose $$\frac{\tau_x}{\rho H}=\tau_0 e^{-y^2/2L^2}$$

$$\rightarrow g^*\frac{\partial h}{\partial x}=\tau_0\left(1+y^2/L^2\right)e^{-y^2/2L^2}$$

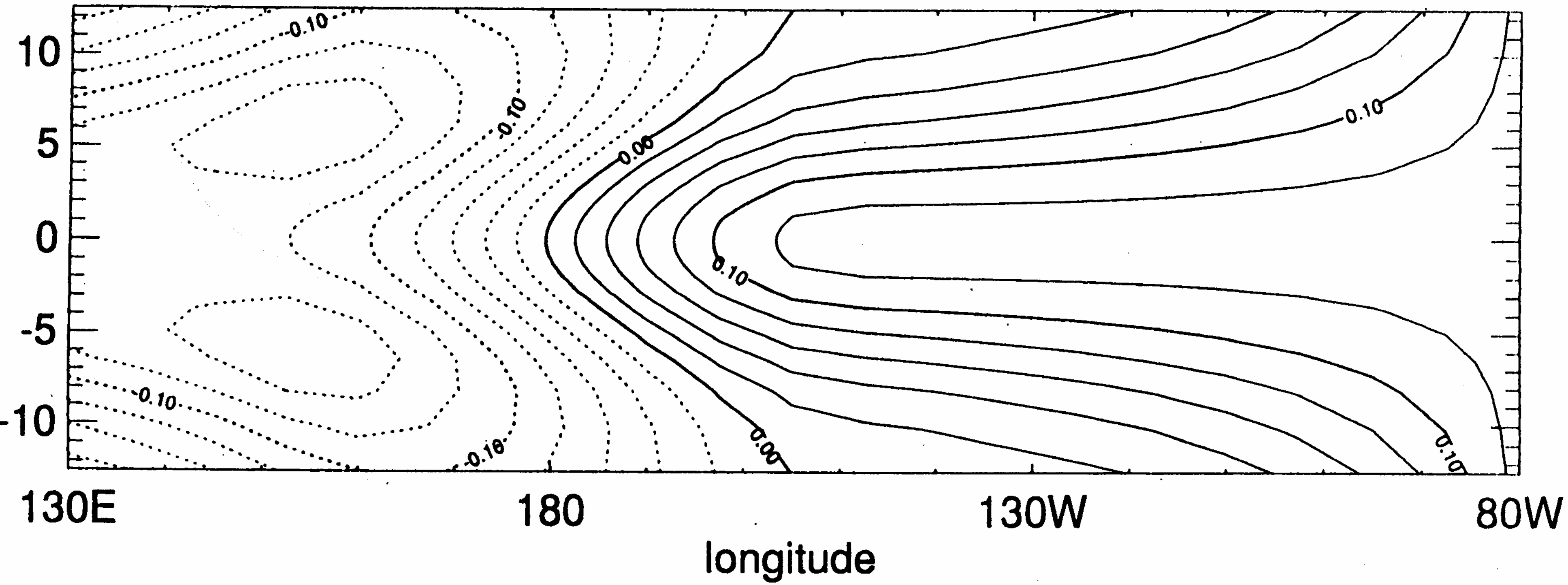

Figure 2. Steady response of thermocline depth in a linear shallow water model to steady wind forcing, constant in latitude. The longitude dependence is a half sinusoid centered on the date line and with half wavelength 60°, zero elsewhere.

Unforced, undamped time-dependent behavior: Same as Matsuno equations in atmosphere:

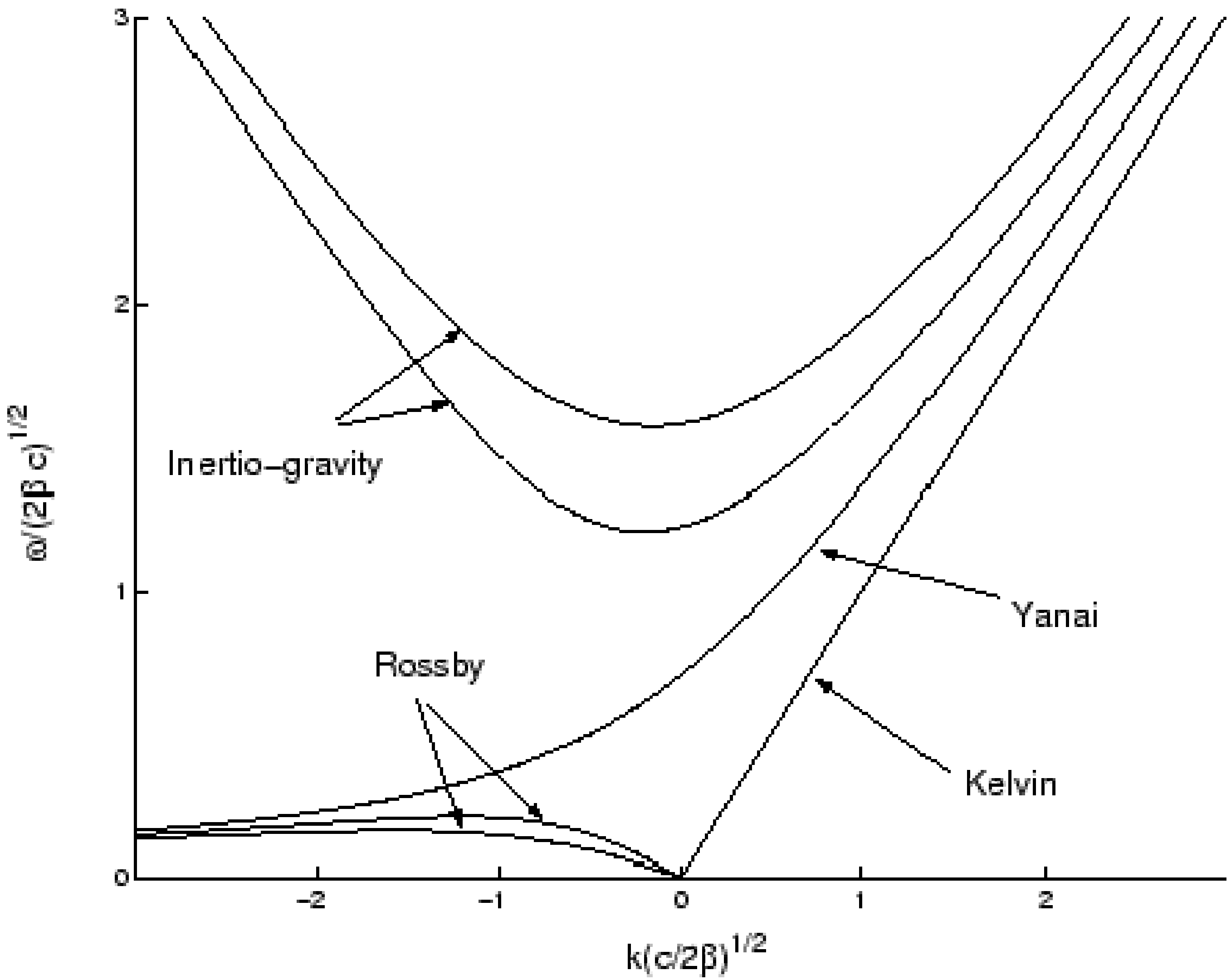

Forced and damped time-dependent solutions for equatorial ocean:

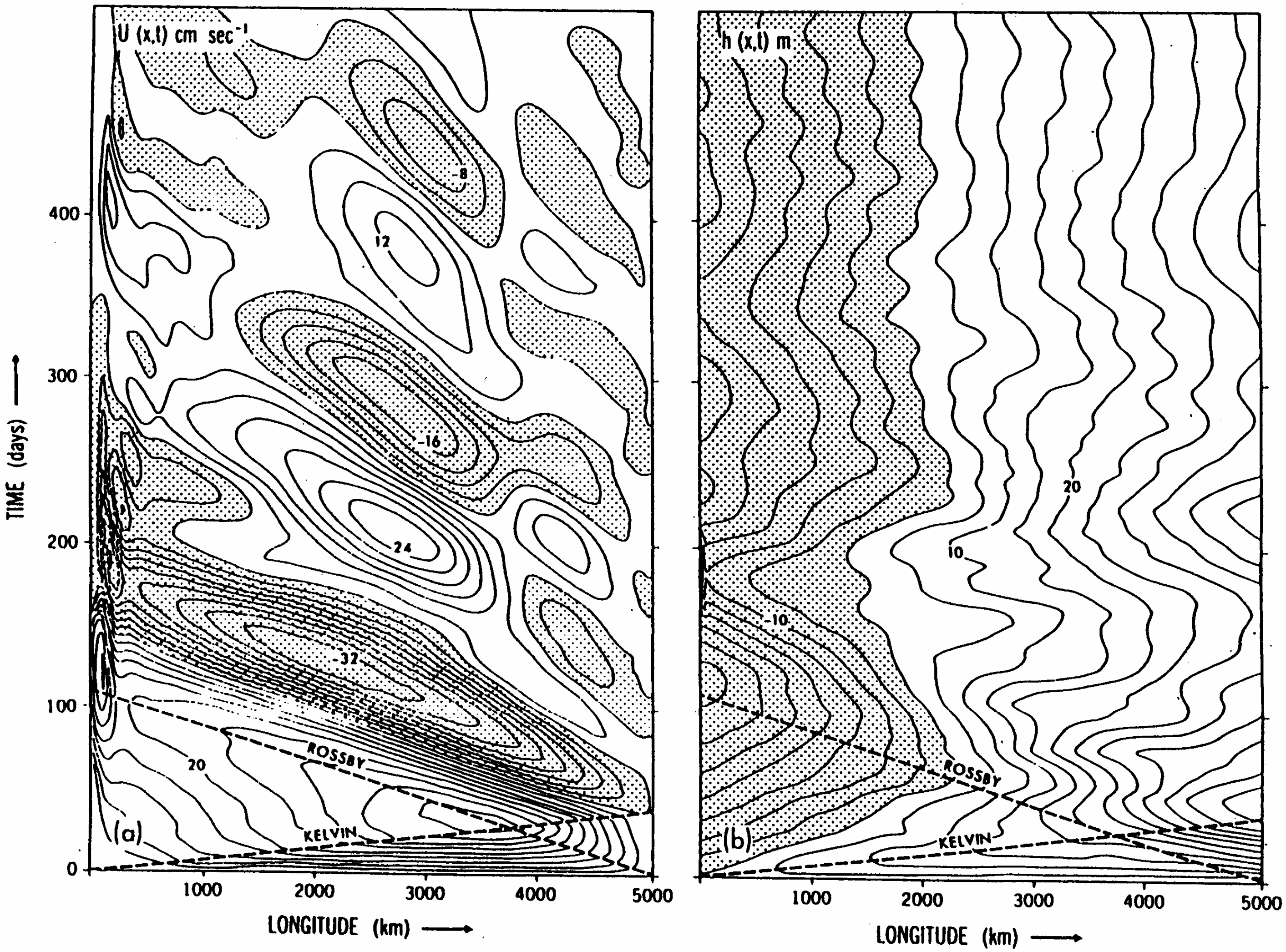

Figure 3.18. Changes in the zonal velocity component (centimeters per second) and in departures from the mean depth of the thermocline along the equator after the sudden onset of spatially uniform eastward winds. The dashed lines indicate the speeds at which Kelvin and the gravest Rossby mode propagate. The thermocline is elevated and motion is westward in shaded areas.

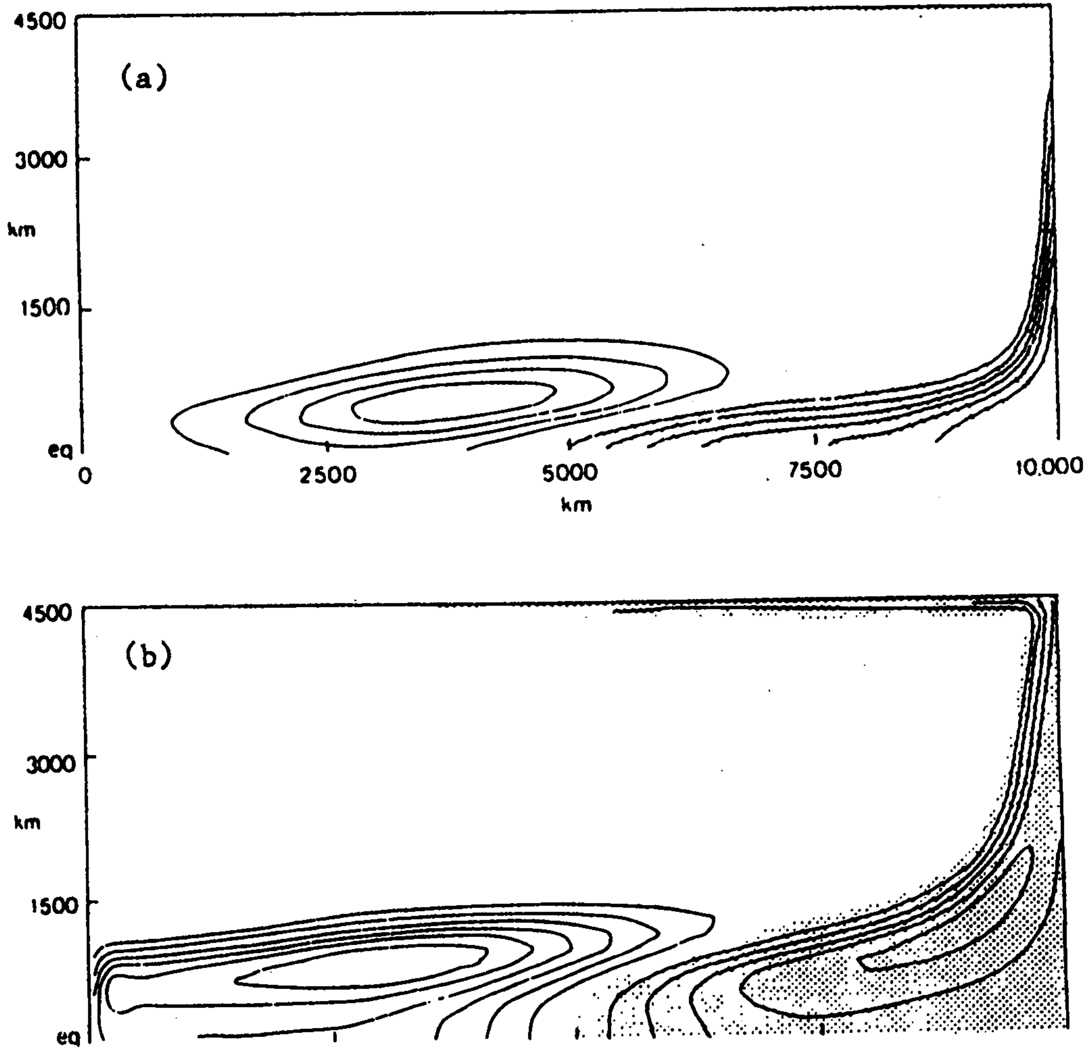

Figure 1. Evolution of thermocline depth in a linear shallow water model following sudden switch-on of a localized wind patch in midbasin. (a) 3 months and (b) 13 months. Months are dimensionalized using wave speeds characteristic of the first baroclinic mode. After *McCreary and Anderson* [1984].

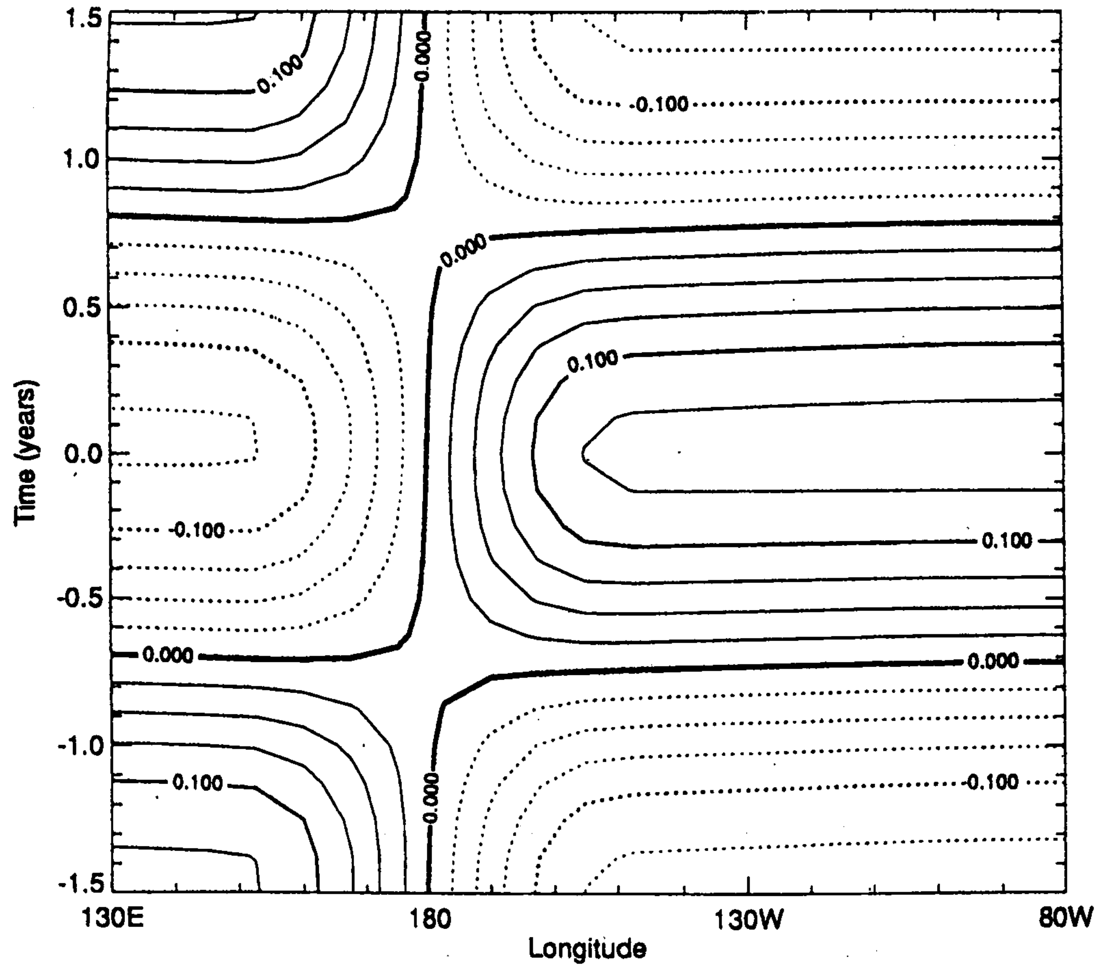

Figure 3. Time-longitude evolution of thermocline depth along the equator from a shallow water model forced by a 3-year period oscillating wind stress path centered at the date line. The calculation is akin to *Cane and Sarachik* [1981], except that the wind stress patch has more ENSO-like longitudinal dependence.

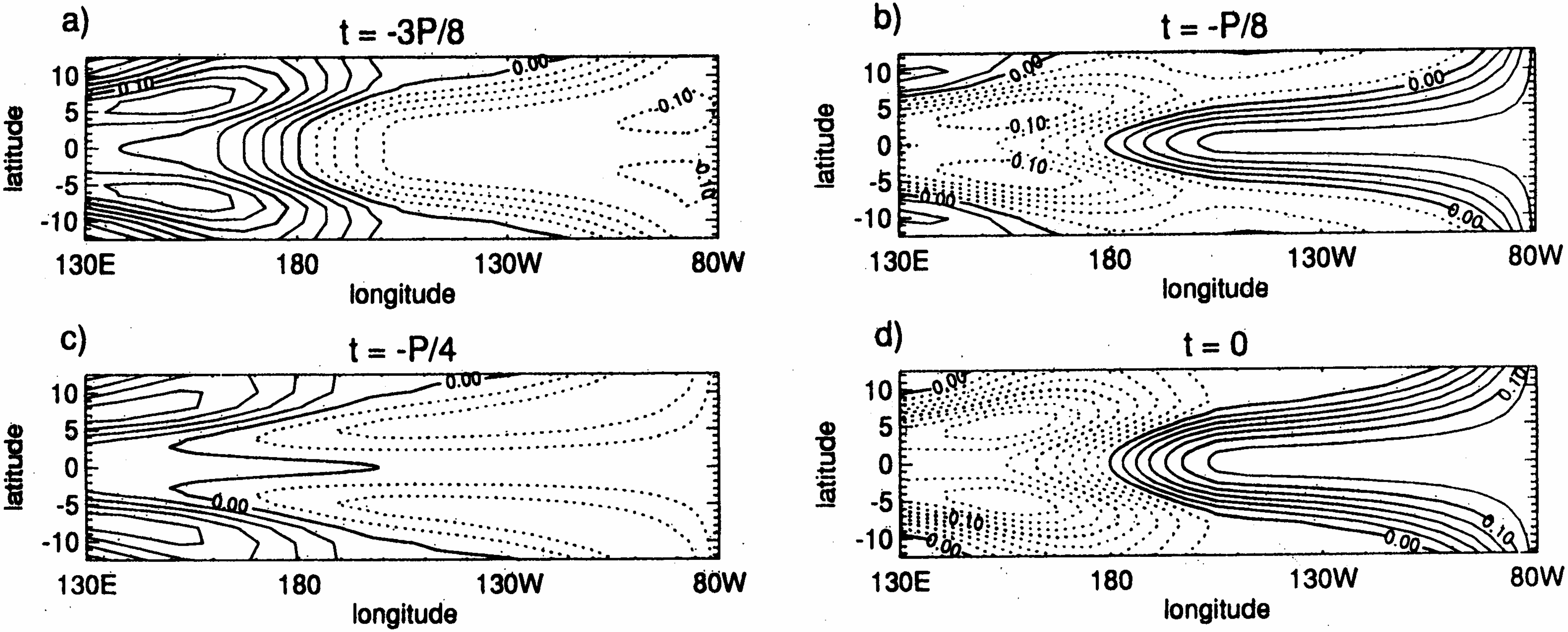

Figure 4. Latitude-longitude evolution of thermocline depth (also proportional to ocean surface height) from a shallow water model forced by the oscillating wind stress patch of period $P = 3$ years, as in Figure 3. Time is indicated in fractions of a period prior to the maximum westerly phase of the winds.

ENSO Theories

- Delayed Oscillator (See E. Tziperman notes)
- Ocean equatorial wave guide (stable or unstable) stochastically forced by atmopshere
- Unstable coupled modes

Rudiments of a local ENSO theory

Consider only (undamped) Kelvin mode in ocean:

$$\frac{\partial u_o}{\partial t} + g^* \frac{\partial h}{\partial x} = \frac{\tau_x}{\rho H},$$

$$\frac{\partial h}{\partial t} + H \frac{\partial u_o}{\partial x} = 0$$

Steady, undamped atmosphere with WISHE, forced by ocean temperature anomalies:

$$\left(T_s - \overline{T}\right)\frac{\partial s^*}{\partial x} = -\beta yv,$$

$$\left(T_s - \overline{T}\right)\frac{\partial s^*}{\partial y} = \beta yu,$$

$$\frac{\partial u}{\partial x} + \frac{\partial v}{\partial y} + \alpha u = -\gamma s_0.$$

$$\alpha \equiv \frac{\varepsilon_p}{1-\varepsilon_p}\frac{C_k \overline{U}}{h|\mathbf{V}|}\frac{\overline{s_0 - s_b}}{\overline{s_b - s_m}}, \quad \gamma \equiv \frac{\varepsilon_p}{1-\varepsilon_p}\frac{C_k |\mathbf{V}|}{H\left(\overline{s_b - s_m}\right)}$$

Eliminate *s** and *v* in favor of *u*:

$$\frac{\partial u}{\partial x} + 2\alpha u + \alpha y \frac{\partial u}{\partial y} = -2\gamma s_0 - \gamma y \frac{\partial s_0}{\partial y}$$

Note that on equator:

$$\frac{\partial u}{\partial x} + 2\alpha u = -2\gamma s_0$$

Surface stress and ocean temperature:

$$\tau_x \cong \rho_a C_D \overline{|\mathbf{V}|} u, \qquad s_0 \cong \mu h$$

Ocean:

$$\frac{\partial u_o}{\partial t} + g^* \frac{\partial h}{\partial x} = \frac{\rho_a C_D \overline{|\mathbf{V}|}}{\rho H} u,$$

$$\frac{\partial h}{\partial t} + H \frac{\partial u_o}{\partial x} = 0$$

Atmosphere:

$$\frac{\partial u}{\partial x} + 2\alpha u = -2\gamma\mu h$$

Eliminate variables in favor of *h*:

$$\left(\frac{\partial}{\partial x}+2\alpha\right)\left(\frac{\partial^2 h}{\partial t^2}-g^*H\frac{\partial^2 h}{\partial x^2}\right)-2\gamma H\mu\frac{\rho_a C_D\overline{|\mathbf{V}|}}{\rho H}\frac{\partial h}{\partial x}=0$$

Scalings:

$$c\equiv\sqrt{g^*H}$$

$$\alpha'\equiv a\alpha$$

$$\chi\equiv 2\gamma H\mu\frac{\rho_a C_D\overline{|\mathbf{V}|}}{\rho H a^2 c^2}$$

$$x\rightarrow ax$$

$$t\rightarrow {}^{a}\!/_{c}\,t$$

$$\left(\frac{\partial}{\partial x}+\alpha'\right)\left(\frac{\partial^2 h}{\partial t^2}-\frac{\partial^2 h}{\partial x^2}\right)-\chi\frac{\partial h}{\partial x}=0$$

$$h=h_0 e^{ikx-i\omega t}$$

$$\omega^2=k^2-\frac{\chi}{1-i\,\alpha'/k}$$

No WISHE (α'=0):

$$\omega^2 = k^2 - \chi$$

Modes are either neutral and propagating (but slowed down by interaction with atmosphere), or stationary and amplifying/decaying.

With WISHE effect (unstable, eastward-propagating modes only when α’ < 0):

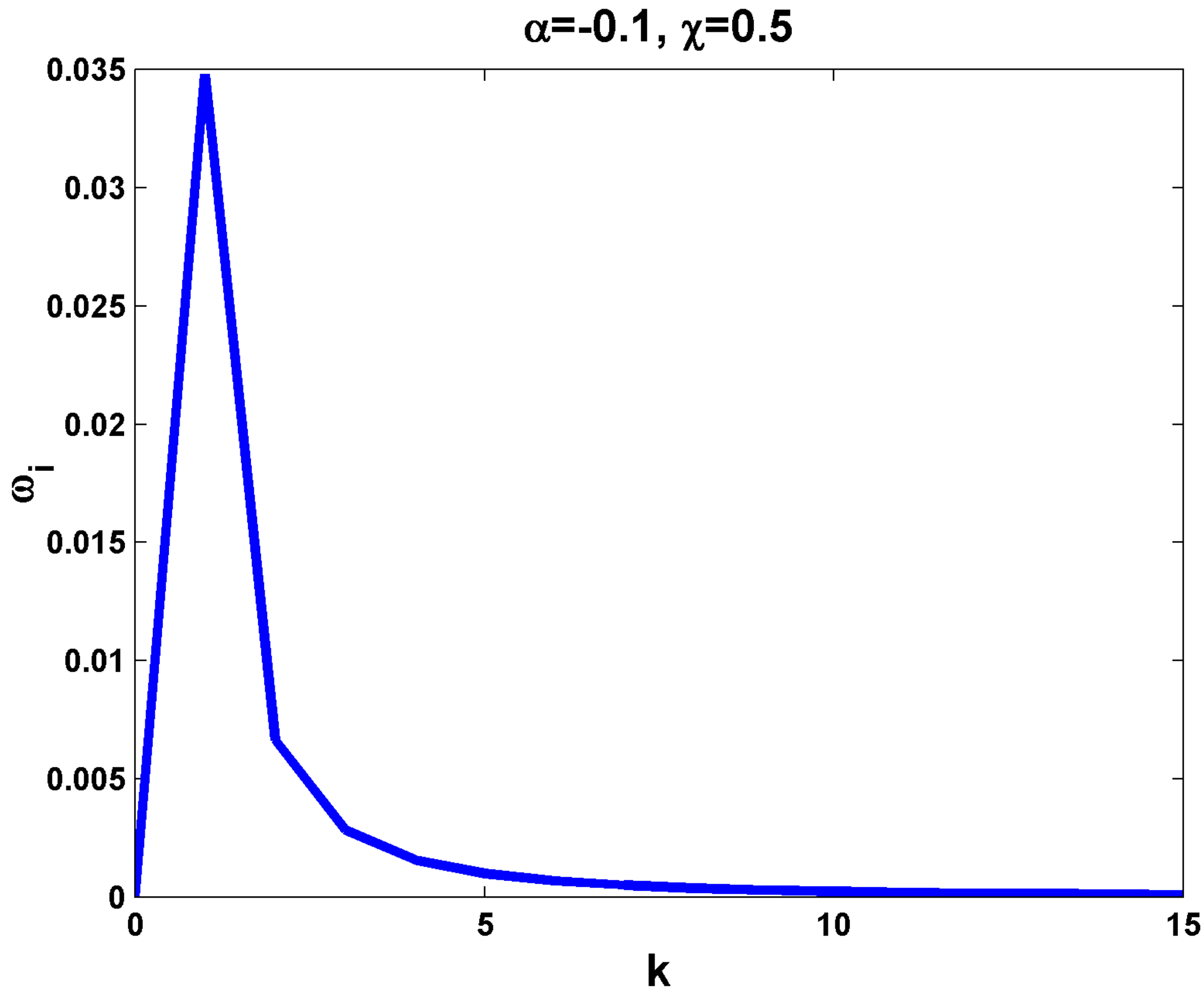

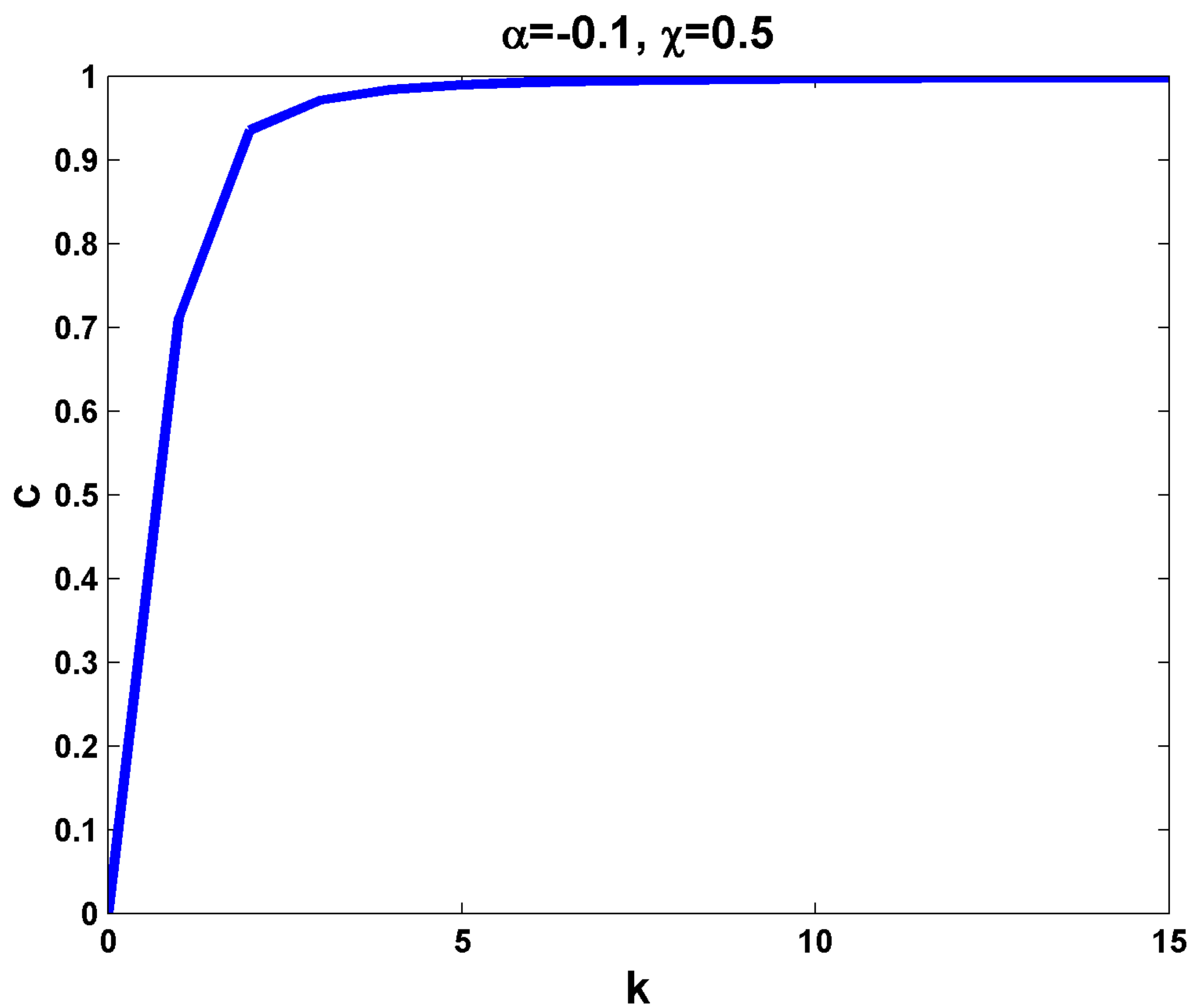
α=-0.1, χ=0.5
c
k
0
0.1
0.2
0.3
0.4
0.5
0.6
0.7
0.8
0.9
1
0
5
10
15

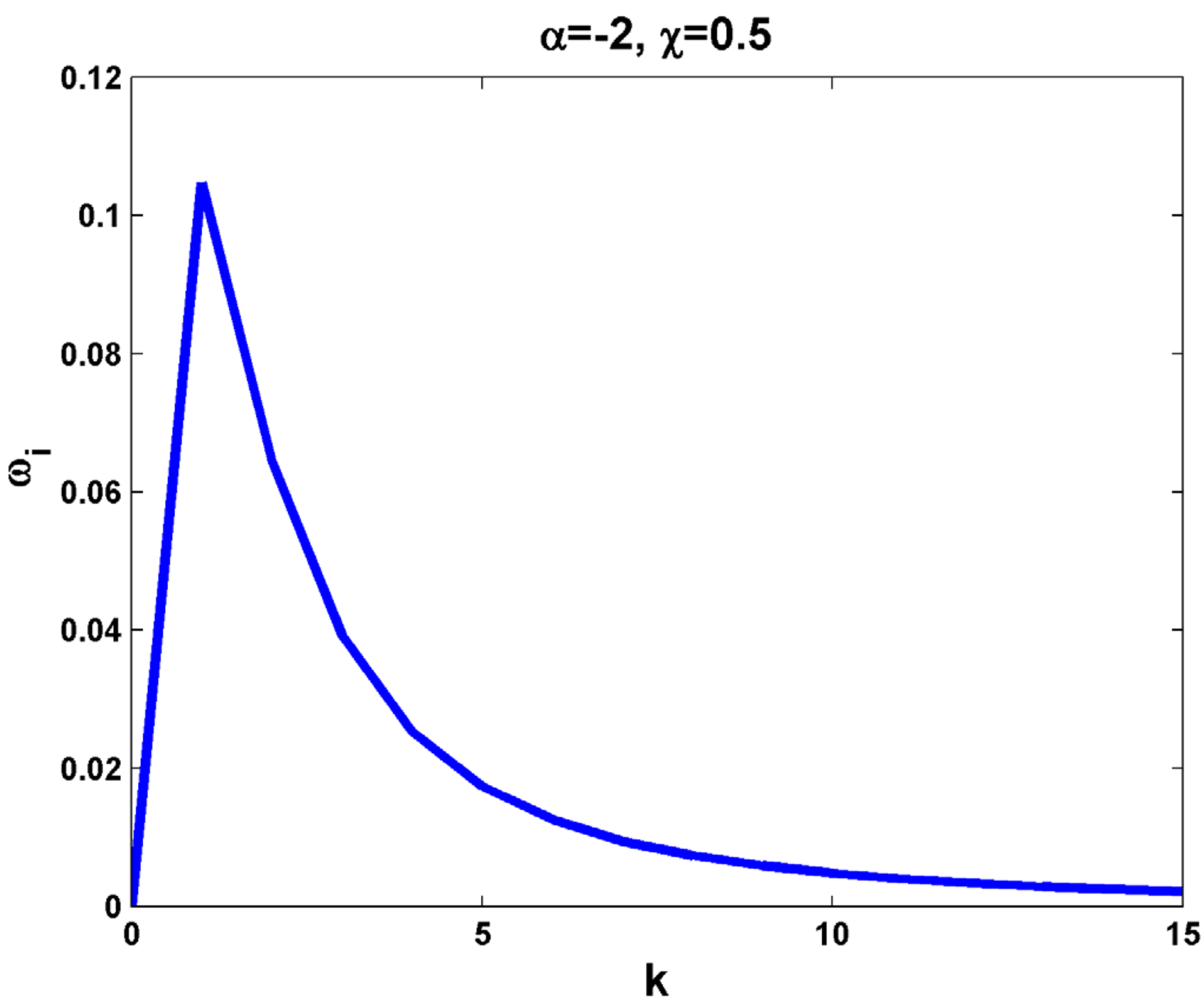
α=-2, χ=0.5
0.12
0.1
0.08
0.06
0.04
0.02
0
ω_i
0
5
10
15
k

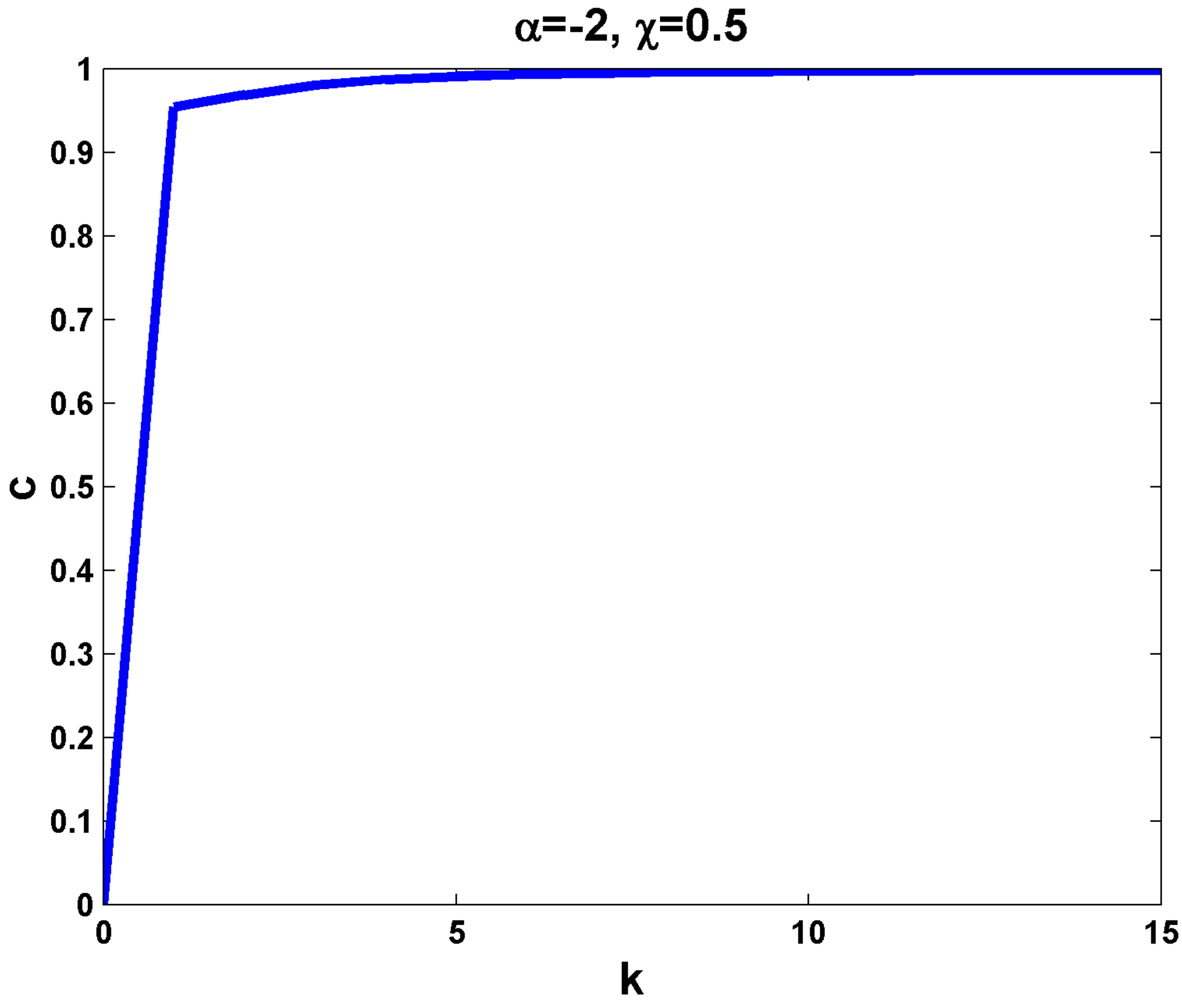

α=-2, χ=0.5
c
k
0
0.1
0.2
0.3
0.4
0.5
0.6
0.7
0.8
0.9
1
0
5
10
15

These are only approximate solutions:

- Coupling produces mismatch of y structure...no pure Kelvin modes in ocean
- Advection of temperature by ocean currents ignored
- Mean slope of thermocline ignored
- No damping terms
- No influence of surface flux variations on ocean temperature

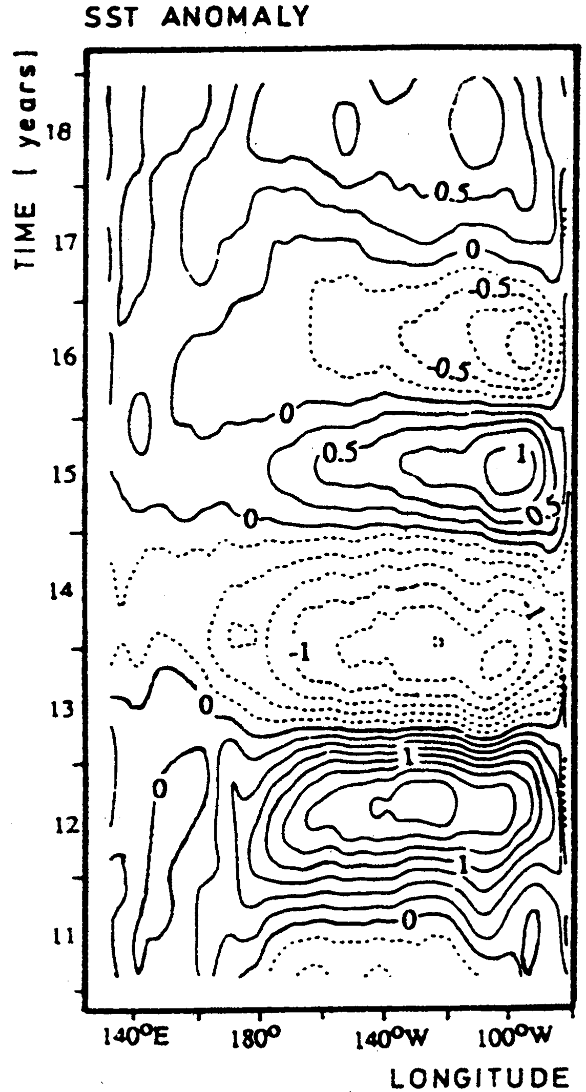

Figure 5 Time-longitude plot of anomalies along the equator from the Philander et al (1992) coupled GCM. (*Left*) SST (contour interval 0.25 C). (*Right*) heat content integrated above 300 m (contour interval 50 C m). After Chao & Philander (1993). The data have been low-pass filtered to remove time scales less than 24 months.

Coupled Models

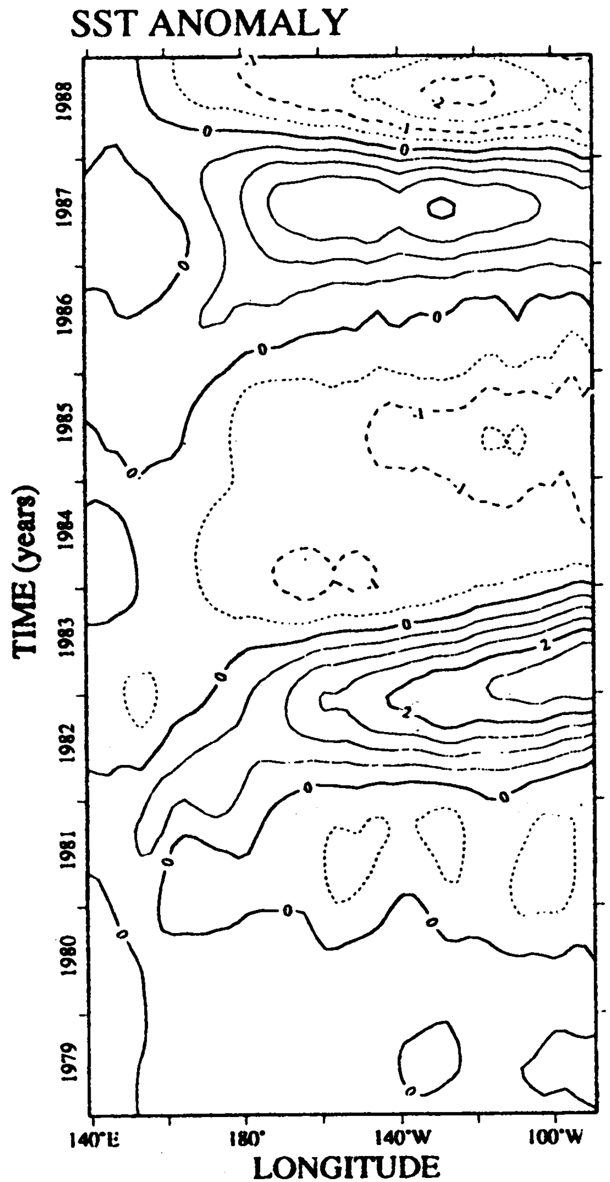

Observed

Figure 3 Time-longitude plot of observed anomalies along the equator. (*Left*) SST (contour interval 0.5 C). (*Right*) heat content integrated above 275 m (contour interval 100 C m). The data have been low-pass filtered to remove variability on time scales smaller than 17 months. Data sets are described in Reynolds (1988) and Barnett et al (1993), respectively.

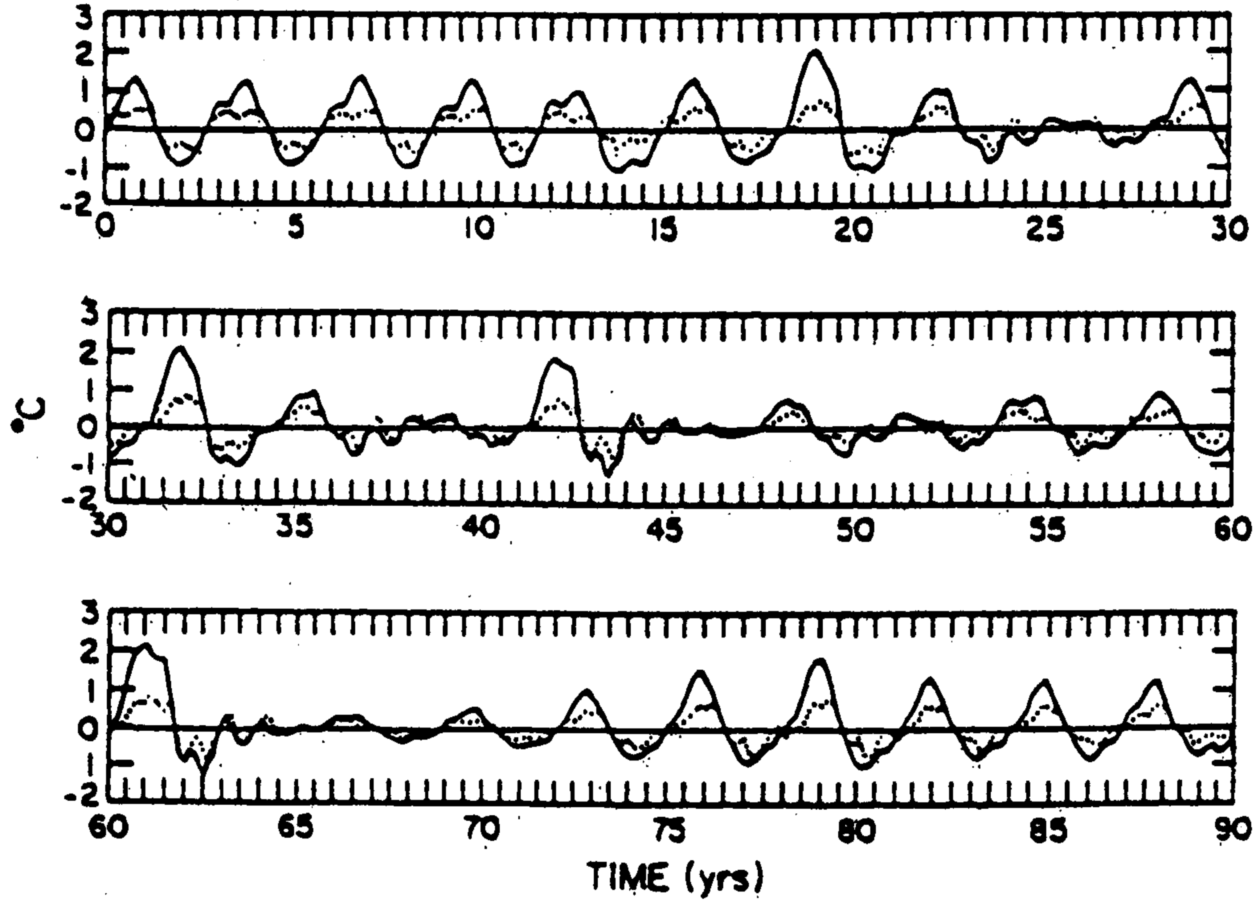

Figure 7. Time series of sea surface temperature anomalies simulated by the *Cane and Zebiak* [1985] intermediate coupled model over 90 years of a coupled model run. The solid line is the "Niño 3" index (SST anomalies averaged 5° N-5°§, 150° W-90° W), the dashed line is "Niño 4" (5° N-5° 160° E-150° W). From *Zebiak and Cane* [1987].